

## CHAPTER 8

### **Crystallization and Multiple Melting Behavior of a New Semicrystalline Polyimide based on 1,3-bis (4-aminophenoxy) benzene (TPER) and 3,3', 4,4'-benzophenonetetracarboxylic dianhydride (BTDA)**

#### **Abstract**

This study addresses the crystallization and multiple melting behavior of a new high temperature semicrystalline polyimide, which is based on an ether diamine (TPER or 1,3 (4) APB) and BTDA dianhydride, both of which are commercially available. It also uses phthalic anhydride to endcap the chains thus improving thermal stability. The polyimide displays a  $T_g$  at ca. 230°C and two prominent melting endotherms at 360°C and 416°C respectively, with a sharp recrystallization exotherm immediately after the lower melting endotherm. The polyimide is able to crystallize even after exposure to high melt temperatures of 450°C (for 1 min) and displays fast crystallization kinetics with cooling rates larger than 200°C/min necessary to quench the polymer into an amorphous state. Additionally, the melting behavior is tremendously influenced by small variations in the melt crystallization temperature. A small melting shoulder appears ca. 10-15°C above the crystallization temperature (for  $T_c \leq 345^\circ\text{C}$ ), while only one prominent higher melting endotherm is observed for  $T_c \geq 350^\circ\text{C}$ . DSC, hot stage polarized optical microscopy and WAXD experiments are utilized to interpret the melting behavior. Indirect evidence suggests that the two prominent melting endotherms are due to different crystal unit cell structures. The prominent multiple melting endotherms represent the melting of primary crystals formed at the crystallization temperature and are not a consequence of a 'continuous' melting and recrystallization process. For temperatures

higher than 350°C, an isothermal thickening phenomenon occurs with significant increases in the peak melting point (10-14°C) observed for longer crystallization times.

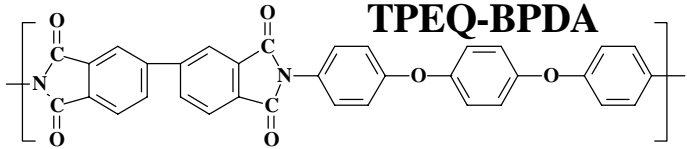
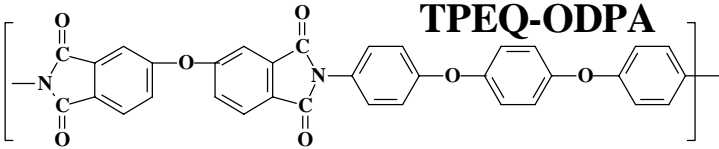
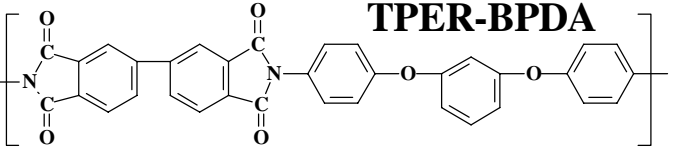
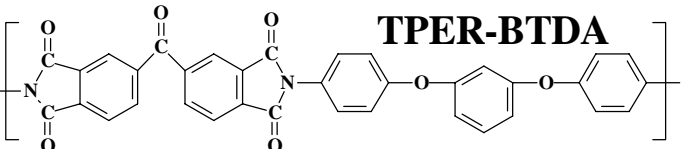
## **8.1 Introduction**

Polyimides are a class of thermally stable and high performance polymers that continue to gain increasing importance in a wide variety of applications like high performance and high temperature adhesives and composites, microelectronics, membranes and as photosensitive materials<sup>1-3</sup>. These wide ranging applications are due to many desirable characteristics generally exhibited by polyimides like excellent mechanical properties, good radiation and chemical resistance, good adhesion properties and low dielectric constant. Presence of crystallinity in these materials can further substantially improve the thermal stability<sup>4-6</sup>, solvent resistance<sup>7</sup>, radiation resistance<sup>8</sup> and partial retention of mechanical properties above the glass transition temperature. In this regard, while many polyimides in the literature have been reported to exhibit crystallinity in the initial material<sup>9,10</sup>, most do not recrystallize once taken to the melt<sup>4-6,11</sup>. The initial crystallinity is in large part due to the solvent aided crystallization which usually accompanies the imidization process, while the usually slow crystallization kinetics prevents the polyimide chain from crystallizing from the melt. Among the few polyimides that do show some evidence of crystallization from the melt, the recrystallization ability decreases rapidly with increasing times and temperatures in the melt. The glass transition temperature of these high temperature polymers is usually in excess of 200°C and the melting points are in the range of 400°C. The melt processing temperatures can thus often exceed 400°C and the poor melt recrystallization behavior can, in part, be explained due to the degradation reactions that can occur at these very high temperatures. Thus it is no surprise that polyimides are almost exclusively processed from the solvent route, which necessitates use of toxic solvents such as N-methyl pyrrolidinone (NMP), N,N- dimethyl formamide (DMF) and dimethyl acetamide (DMAc) among others. Additionally, these solvent aided processes are more time consuming and expensive than the traditional melt processing operations. It is therefore obvious that development of melt processable thermoplastic polyimides can be beneficial

from both an environmental and processing standpoint. With this aim in mind, several semicrystalline polyimides have been synthesized and characterized<sup>4-6,11</sup>, some of which are shown in Table 1. Additionally, all these polyimides are based on commonly available dianhydrides and ether diamines and thus no separate synthesis step is required to prepare the monomers. Each of these polyimides show crystallinity in the initial material, a high glass transition and a high melting temperature. However, depending upon small differences in their structure, the success in terms of their melt crystallization behavior varies. Incorporating flexible ether or carbonyl linkages in the dianhydride and changing the nature of isomeric attachment in the diamines influences the melt crystallization behavior significantly. In earlier work from this laboratory, it has been shown that TPEQ-ODPA shows limited recrystallizability from the melt<sup>12</sup>. It was also found that the polyimide TPEQ-BPDA demonstrated a very high DSC peak melting point of 471°C and did not recrystallize once taken to the melt<sup>11</sup>. The third polyimide TPER-BPDA, however, has provided excellent results from the viewpoint of melt recrystallization. Earlier works have shown the excellent thermal stability and melting characteristics<sup>4,5</sup>, crystallization and morphological behavior<sup>4-6</sup>, fast crystallization kinetics<sup>6</sup>, rheological behavior<sup>6</sup> and very promising adhesive strengths and durability of this polyimide<sup>4</sup>. The work reported in this chapter introduces another new semicrystalline polyimide (polyimide (d) in Table 1) based on 1,3-bis (4-aminophenoxy) benzene (TPER or 1,3(4) APB) and 3,3', 4,4'-benzophenonetetracarboxylic dianhydride (BTDA). The polyimide henceforth referred to as TPER-BTDA displays a  $T_g$  of ca. 230°C and two prominent melting endotherms with peak melting points of ca. 350°C and 410°C. Additionally, the chains are endcapped with phthalic anhydride that serves to control the molecular weight and tremendously improves the thermal stability of the polyimide.

Several reasons for synthesizing the present polyimide exist. Traditionally BTDA based polyimides have been found to be promising with respect to their crystallization behavior. Also, an earlier study dealing with this polyimide seemed to indicate that this material may crystallize from the high melt temperatures<sup>13</sup>. Changing the dianhydride structure to BTDA also helps in better understanding the structure property behavior in these ether diamine based semicrystalline polyimides. Additionally BTDA

**Table 8.1** Previously developed semicrystalline polyimides developed at Virginia Tech.

	M.W. (daltons)	T <sub>g</sub> (°C)	T <sub>m</sub> (°C)
 <p><b>TPEQ-BPDA</b></p>	550	259	471
 <p><b>TPEQ-ODPA</b></p>	550	238	420
 <p><b>TPER-BPDA</b></p>	566	210	395
 <p><b>TPER-BTDA</b></p>	578	230	416

based polyimides are more attractive from the commercial viewpoint due to the lower cost of BTDA vis a vis other dianhydrides. The present study deals with the crystallization from the melt and the multiple melting behavior of TPER-BTDA polyimide. A subsequent study will also address the thermal stability, morphology and dynamic mechanical behavior of this polyimide.

The DSC melting behavior of this semicrystalline polyimide is particularly interesting in that it demonstrates two very distinct and widely spaced melting endotherms at ca. 350°C and at ca. 410°C. Also, as will be subsequently shown, additionally endotherms develop depending upon the temperatures at which the polymer is crystallized. It is very important from both a fundamental and practical standpoint to understand the causes of this multiple melting behavior and how it may depend upon the previous thermal history of the polyimide. While such widely spaced distinct melting endotherms with a prominent intermediate crystallization exotherm have not commonly been observed, the problem of multiple melting behavior in semicrystalline polymers itself is not new. Multiple melting behavior has been observed in polyethylene<sup>14-17</sup>, polypropylene<sup>18-20</sup>, poly(ethylene terephthalate) (PET)<sup>21-27</sup>, poly(butylene terephthalate) (PBT)<sup>28-33</sup>, poly(phenylene sulfide)<sup>34,35</sup>, poly(ether ether ketone) (PEEK)<sup>36-55</sup> semicrystalline polyimides<sup>5,56-61</sup> and other polymers. The multiple melting behavior itself can occur due to a wide variety of reasons like different crystal unit cell structures, presence of two or more distinct morphological forms or due to a continuous melting and recrystallization process. Other reasons presented in literature include molecular weight fractionation<sup>17</sup>, dependence on the heating rate in the DSC<sup>62</sup> and ascribing the lower endotherm to some sort of a physical aging process<sup>45-47</sup>. In recent years, considerable debate has re-arisen over the reasons for dual melting behavior observed in PEEK and other polymers. The two widely advocated models for explaining the melting behavior differ in that one proposes a melting-recrystallization process while the other explains it on the basis of two different lamellar populations. For the melting recrystallization process, the lower endotherm has been argued to be due to melting of the lamellae that form at the crystallization temperature, while a continuous recrystallization and melting process ensues simultaneously with the higher endotherm occurring when melting rate

sufficiently exceeds the recrystallization rate. One of the several forms of evidence that is cited to support this description is the shifting of the lower peak to higher temperatures and more importantly, the higher peak to lower temperatures, with increase in heating rate. For quiescent crystallization, the *morphological model* (a terminology used often in literature) explicates the dual-melting behavior on the basis of dual lamellar populations, the thicker lamellae being formed due to the primary crystallization while the later forming thinner lamellae are due to the secondary crystallization process. The higher melting point is then ascribed due to the thicker primary lamellae while the lower endotherm, which usually occurs 10-25°C above the crystallization temperature, is the result of the thinner secondary lamellae. One of the stronger evidences cited to support this model is that the higher melting endotherm appears to form first whereas the lower melting endotherm appears later. However, within the proponents of the ‘morphological model’, debate still exists as to the location of thinner lamellae. While some have argued for the existence of thinner lamellae within the stacks of thicker primary lamellae, others have postulated the existence of separate stacks of thinner lamellae<sup>43,48,51</sup>.

This study addresses the crystallization and multiple melting behavior of this polyimide by using the techniques of DSC, optical microscopy and wide angle X-ray diffraction (WAXD). The polyimide is first introduced by showing some evidence concerning the thermal stability and recrystallization ability from the melt. Thereafter, the effects of crystallization temperature on the melting behavior are discussed. Regarding the kinetics of crystallization, while the detailed quantitative methods like Avrami analysis are not utilized in the present study, some qualitative arguments are made on the basis of the observed results. Reasons for the multiple melting behavior and how this behavior may depend upon the previous crystallization temperature are explained on the basis of the evidence obtained. In this regard, experimental evidence is discussed in order to explain the multiple melting behavior on the basis of different crystal unit cell structures, the ‘melting and recrystallization model’ and the ‘morphological model’. Results of the DSC experiments are shown for the isothermal crystallization for varying times at selected crystallization temperatures. Also, the effect of heating rate on the melting behavior when crystallized at these temperatures is discussed. Lastly, some results are presented regarding the isothermal thickening

phenomenon at relatively higher crystallization temperatures. The problem of estimating the equilibrium melting point using traditional methods is also discussed.

## **8.2 Experimental**

### 8.2.1 Synthesis:

1,3-bis(4-aminophenoxy) benzene (TPER diamine) was supplied by Ken-Seika and was recrystallized from toluene before use. 3,3',4,4'-benzophenonetetracarboxylic dianhydride (BTDA) was supplied by the Occidental Chemical Corporation and was dried at 120°C prior to use. The endcapper phthalic anhydride (PA) was obtained from Aldrich and sublimed prior to use. N-methylpyrrolidinone (NMP) was obtained from Fisher and vacuum distilled after drying over P<sub>2</sub>O<sub>5</sub> before use. The Carothers equation was utilized to calculate the monomer and endcapper concentration for synthesizing polymer samples with the desired number average molecular weight of 30,000 (30K) daltons. The reaction vessel was a three neck round bottom flask equipped with a mechanical stirrer, nitrogen inlet and a drying tube. Sufficient NMP was added to achieve a 10% solids concentration and the solution was allowed to stir for 24 hours, to afford a homogenous poly(amic acid) solution as shown in Figure 8.1. A stepwise thermal imidization procedure was utilized which others as well as workers in this laboratory has used successfully in the past<sup>4</sup>. The first step was the casting of the poly(amic acid) precursor on the pyrex glass plates. These plates were placed in the vacuum oven overnight until smooth non-tacky films were obtained. Thermal imidization was achieved by raising the temperature to 100°C, 200°C and 300°C and holding at each of these temperatures for 1 hour. The time to go from one temperature to the next was ca. one hour each at the fastest heating rate available with the oven. After the completion of the cycle, the plates were allowed to cool down to room temperature before being removed from the oven. The films were carefully stripped off the glass plates in hot water and stored in a desiccator before use.

## Synthesis of TPER-BTDA-PA

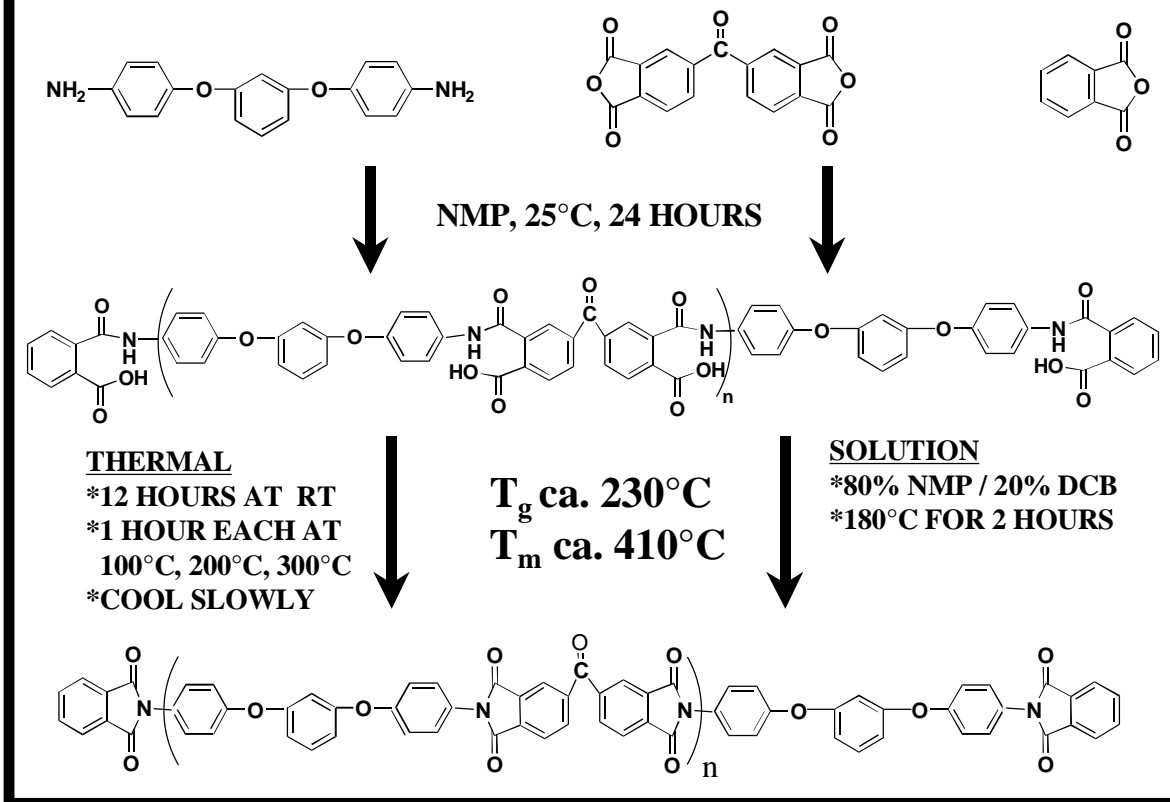


**Figure 8.1** Scheme for synthesis of TPER-BTDA-PA polyimide.



## 8.2.2 Characterization

Thermogravimetric (TGA) studies utilized a Seiko TG/DTA and all experiments were carried in either a nitrogen or air atmosphere. The temperature was calibrated using indium and zinc standards and the dynamic experiments utilized a heating rate of 5°C/min. The isothermal experiments were performed for a duration of 180 minutes.

DSC experiments for both isothermal and non-isothermal crystallization were performed on a Perkin Elmer DSC-7. The amount of polymer utilized in a given thermal scan was kept between 6-8 mg. The DSC was calibrated with indium and zinc standards. All experiments were conducted under a nitrogen purge and a DSC baseline was determined by running empty pans. For isothermal crystallization experiments, the samples were kept at room temperature and purged with nitrogen for 5 minutes to remove air from the DSC cell. The samples were then rapidly heated to 450°C for 1 minute while cooling to below the glass transition temperature was done at the desired cooling rate or to the specific crystallization temperatures at 300°C/min. In this regard, data collection at high supercoolings was hampered by the initial instability of the DSC signal. This initial instability occurs on cooling to the crystallization temperature at fast cooling rates and may persist for ca. one minute on Perkin Elmer DSC 7 utilized in this study. To perform quantitative analysis like Avrami analysis or to calculate the value of  $t_{1/2}$  (time to attain 50% of its total crystallinity), some extrapolation of the initial portion of the exotherm is then usually undertaken (for the higher supercoolings), which results in some degree of error in the final result. In this study however, the peak time for the crystallization exotherm  $t_m$  for various crystallization temperatures is only reported. These values behave similarly as the quantitatively more precise  $t_{1/2}$  parameter and give a good indication of the crystallization kinetics at various supercoolings. For the variable heating rate studies, the DSC was first calibrated using zinc and tin standards at that heating rate using the onset of the melting points. For heating rates higher than 10°C/min, the sample mass was reduced to 2-3 mg to minimize the thermal lag that may

result at higher heating rates. All experiments were performed twice in order to maintain accuracy in the results. All reported DSC scans are normalized with respect to the sample mass (to 1 mg).

Polarized optical microscopy was carried out on a Zeiss optical microscope equipped with a Linkam 600 hot stage and 35mm camera. The hot stage was calibrated using indium, tin and zinc. The film (~2 mils) was sandwiched between two glass slides and a nitrogen purge was maintained inside the hot stage. The sample was taken to 450°C and kept there for 1 minute before being quenched to a 340°C, kept there for 20 minutes and then rapidly heated to and held at 370°C. The quenching to 340°C from 450°C was achieved by using a separate nitrogen source.

For wide angle X-ray diffraction experiments, a Siemens diffractometer equipped with a STOE Bragg-Brentano type goniometer was utilized. A wavelength of 1.54 Å was used after monochromitization through a graphite monochromator. Data was collected during a continuous scan at a speed of 0.5 degrees/minute between the angles of 10°-60°.

### **8.3 Results and discussion**

Thermogravimetric analysis was first utilized to determine the thermal stability of the material as indicated by weight loss that may occur at higher temperatures. Dynamic experiments at a slow heating rate of 5°C/min were conducted from room temperature to 600°C in both air and nitrogen environments (Figure 8.2(a)). The 5% weight loss temperatures in air and nitrogen are 507°C and 529°C respectively. It is clear that the polymer exhibits significantly higher thermal stability in nitrogen than in air, as the onset of degradation accompanied by significant weight loss appears to start in air at lower temperatures. These high weight loss temperatures are not surprising and are usually obtained for such high temperature thermally stable polyimides. However, before weight loss temperatures are utilized to compare thermal stability of any two materials, it is important to recognize that the exact value of such temperatures would depend significantly on the heating rate utilized. For the higher and commonly utilized heating

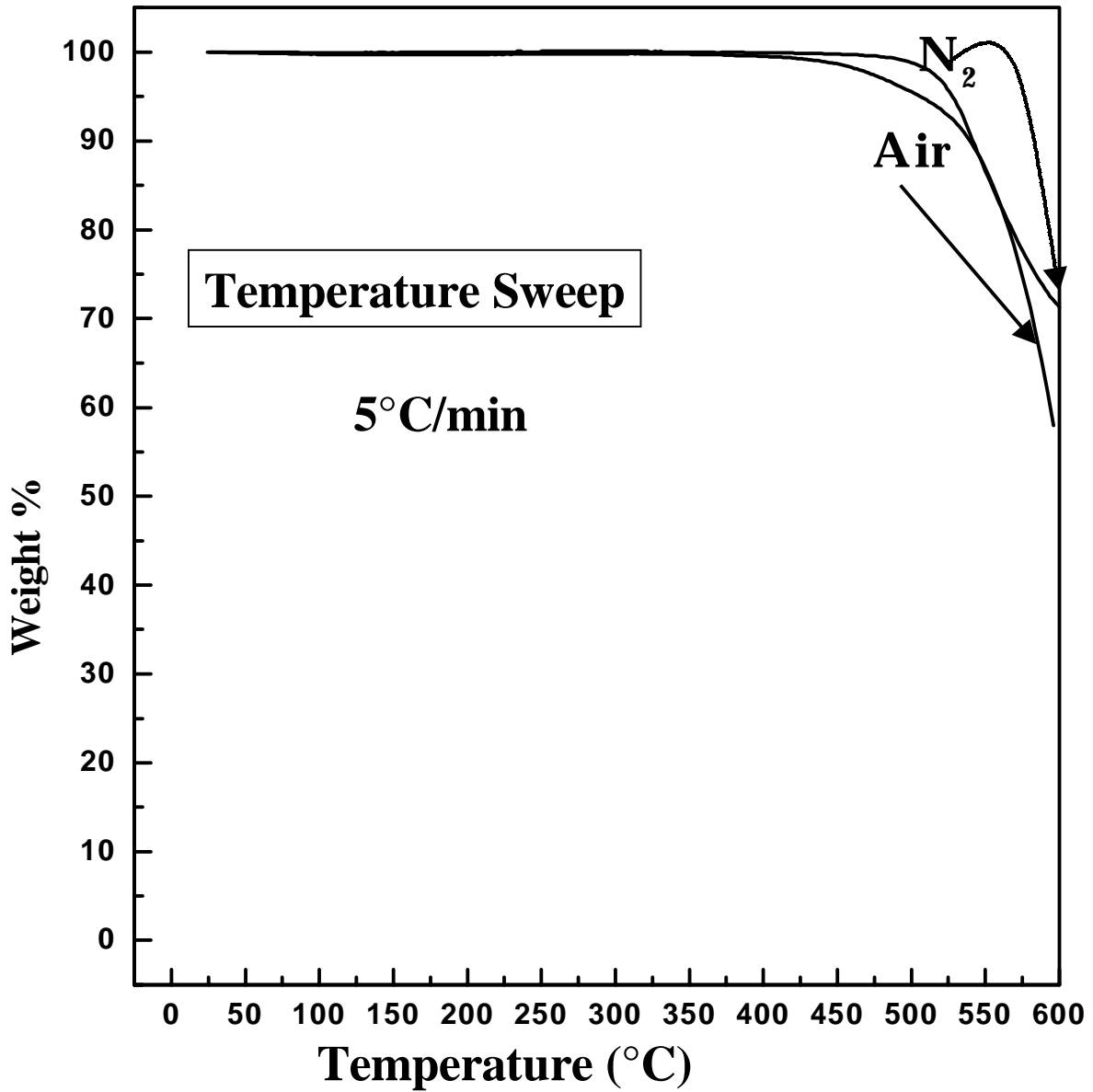


**Figure 8.2(a)** Dynamic heating profiles for weight loss in air and nitrogen when heated at 5°C/min.

rate of 10°C/min, the weight loss temperatures would obviously be higher as the polymer spends less time at any temperature. Similarly for a low heating rate of say 2°C/min, the weight loss temperatures may be significantly lowered due to the increased time spent at the previous temperatures.

While the degradation temperatures obtained in (at 5°C/min) are higher than the possible melt processing temperatures of ca. 450°C, it is important to understand the effect of prolonged exposure at melt processing temperatures. In this regard, the isothermal scans for weight loss vs. residence time in the melt, at a typical melt temperature of 450°C are shown for both in air and nitrogen (Figure 8.2(b)). While the weight loss begins to occur in air for low residence times, the polyimide shows very little weight loss even after 180 minutes in the melt at 450°C. The 5% weight loss time in air is 56 minutes, while 4.7% weight loss occurs in 180 minutes in nitrogen.

While the above traditionally utilized TGA experiments reveal the significant bulk thermal stability with respect to weight loss for this polyimide, no major inference can be made regarding the recrystallizability of the material from these temperatures. While TGA would detect the weight loss due to degradation reactions that are accompanied by emission of volatiles, other less severe reactions like crosslinking/chain branching may take place with little or no emission of volatiles, and thus little observable weight loss. These reactions, however, may significantly inhibit the ability of the material to crystallize from the melt. The increased viscosity that may result due to these reactions would also make the melt processing of the polymer difficult. Hence, TGA experiments, while serving as a gross measure of thermal stability, are of limited utility from understanding the stability from a recrystallization viewpoint.

To understand the initial melting behavior and recrystallization response once heated above the melting temperature, DSC experiments were conducted by heating the polymer to the melt temperature of 450°C for 1 minute and rapid quenching to below the glass transition temperature. The four consecutive scans are shown in Figure 8.3. The initial material, which is crystalline, shows only a weak and broad glass transition in the vicinity of 230-260°C. However, very interestingly, two prominent and widely spaced melting endotherms, with peak temperatures of 357°C and 416°C respectively are

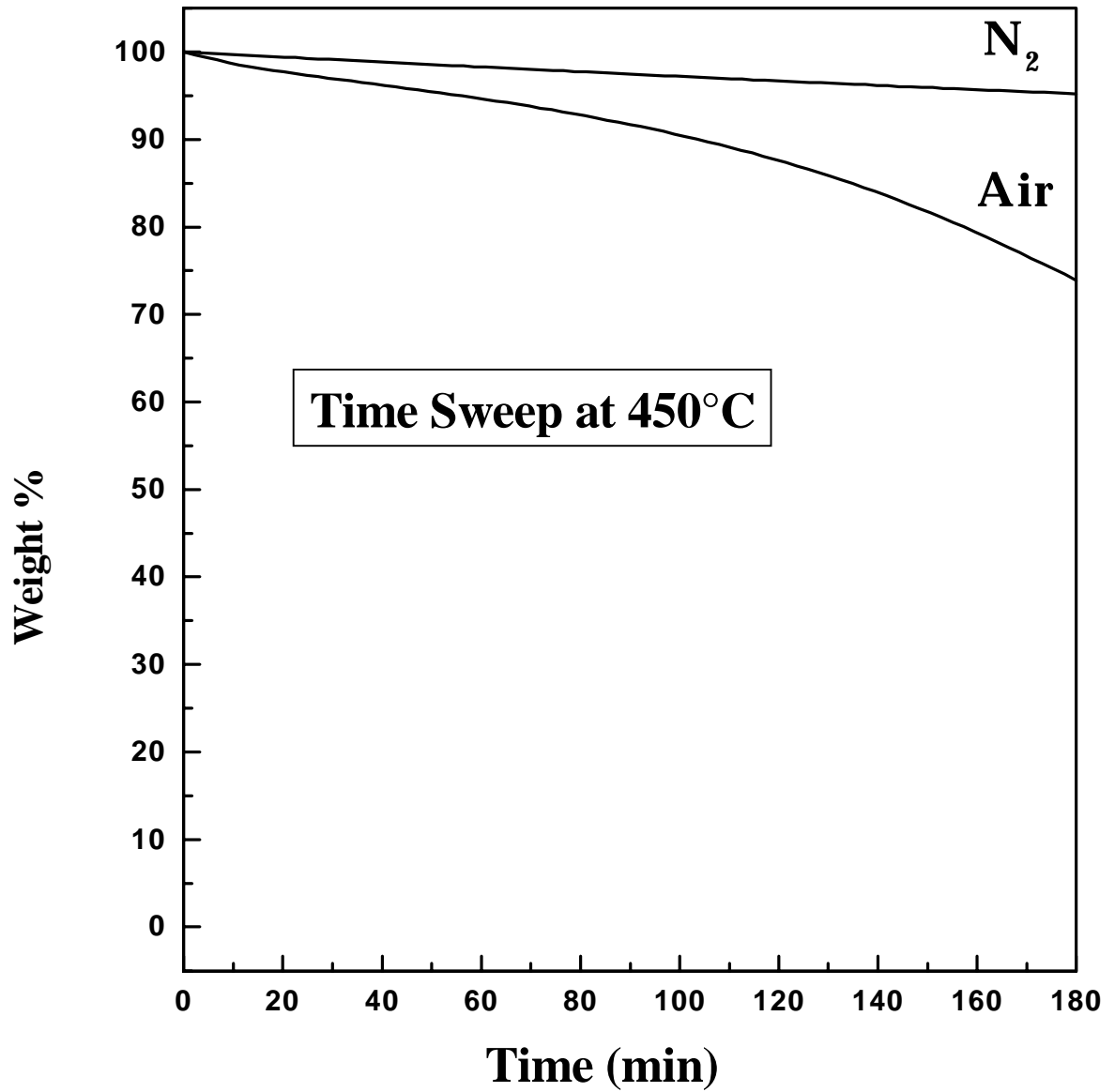


**Figure 8.2(b)** Weight loss profile with time in air and nitrogen when kept at a typical melt temperature of 450°C/min.

observed. The first melting endotherm is also rapidly followed by a recrystallization exotherm, which lies between the two melting endotherms. Such peculiar melting behavior has not often been observed for other semicrystalline polymers. It is also noticed that in the initial material, the higher melting endotherm is significantly larger than the lower melting endotherm.

Figure 8.3 also shows consecutive heating scans once the polyimide is *quenched* from the melt. In this regard, several features are observed, mainly:

- (1) The glass transition temperature becomes clearer (in terms of a narrow well-defined heat capacity jump) occurring at 230°C. The  $T_g$  is maintained for all the consecutive scans.
- (2) A prominent crystallization exotherm ca. 20°C above the  $T_g$  appears. The peak temperature of this exotherm shifts to slightly higher temperatures with consecutive scans. The relative magnitude however, does not change much.
- (3) The peak of the lower melting endotherm shifts downward to 347°C and both this peak temperature and the relative magnitude of this lower endotherm are maintained for the consecutive scans.
- (4) The recrystallization exotherm continues to appear after the first endotherm, and shifts slightly to higher temperatures accompanied with moderate decrease in size. The higher melting endotherm continues to decrease in size and shifts to lower temperatures with repeat heating.

For the consecutive heating scans, the overall heat of melting (as given by ‘area under the endotherms-area under the exotherms’) is close to zero, thus indicating that it was possible to quench the polymer to nearly an amorphous state from the melt. The well-defined  $T_g$  thus results from the removal of the constraints that were provided by the crystallites in the initial material. *The polyimide though, did not loose its ability to rapidly crystallize as evidenced by the crystallization exotherm just above the  $T_g$ .* However, the shift of this exotherm to higher temperatures with successive scans indicates that more thermal energy is required to introduce crystallization. This could possibly be in part the result of a small amount of crosslinking/chain branching reactions that may occur every time the polyimide is heated to 450°C for 1 minute. Such short

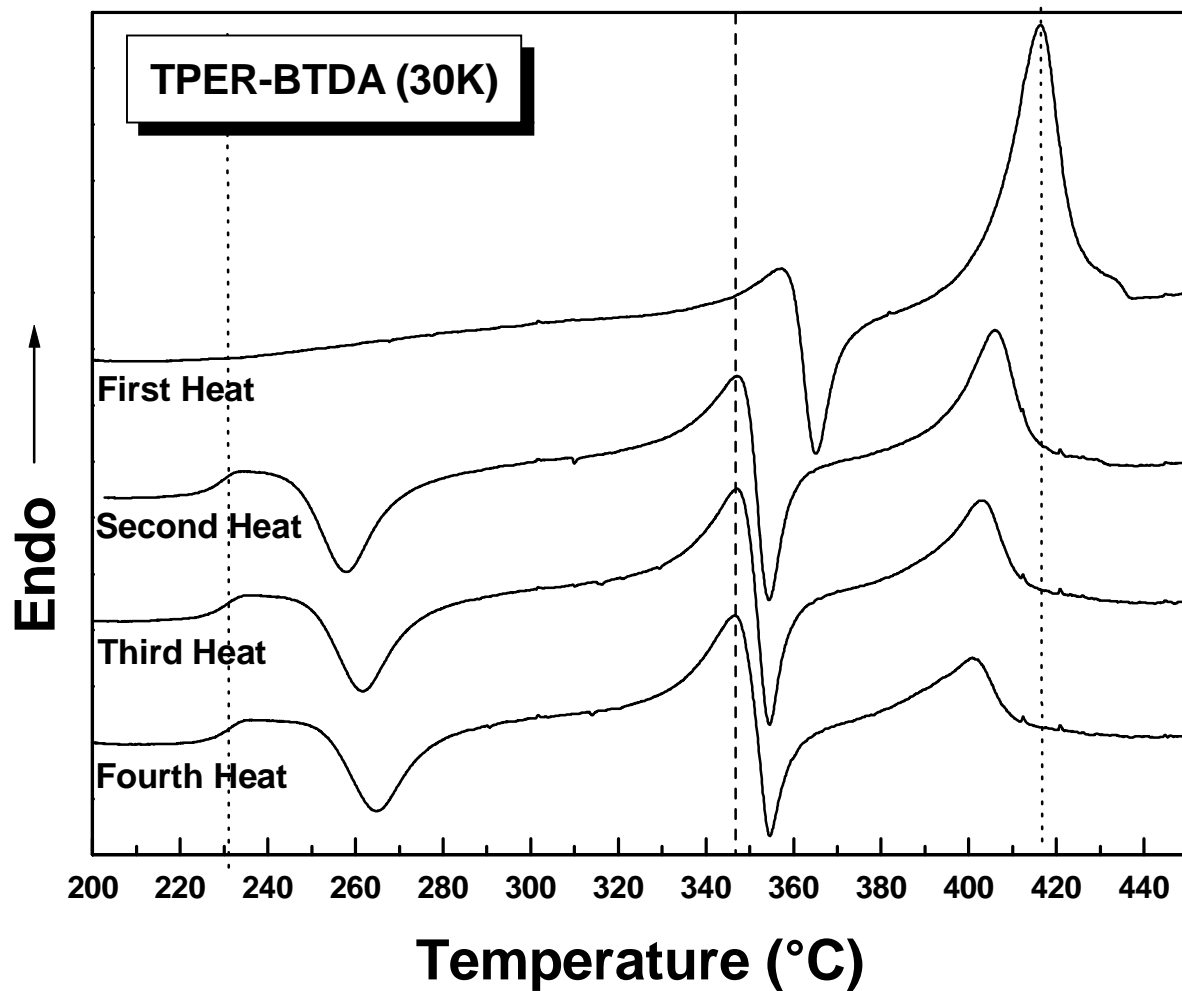


**Figure 8.3** Consecutive DSC heating scans after heating to 450°C at 10°C/min, holding for 1 min, quenching to 100°C and reheating at 10°C/min.

time exposures though do not result in any observable weight loss, as already discussed previously. If any large-scale crosslinking reactions had occurred than the polyimide's ability to crystallize would be severely hampered, resulting in little or no crystallization during the heating scan. All experiments discussed henceforth in this chapter will only utilize the milder melt conditions of 450°C for 1 minute.

The construction of a baseline extending from just above the glass transition temperature to the end of the melting enables the calculation of the relative amount of crystal content associated with the respective crystallization exotherms and the melting endotherms. However, exact values are not tabulated here as results depend on slight variations in the placement of the baseline (due to the nature of the DSC curves). Nonetheless, some characteristics of the melting behavior are evident. Both the higher and lower melting forms are present in the initial material as the heat of melting associated with the higher temperature peak is clearly greater than the heat of crystallization of the intermediate exotherm. However, for the later scans, these amounts are nearly equal indicating that the higher melting form is primarily the result of recrystallization occurring after the lower melting endotherm. The lower melting form in this case is mainly the result of melting of the crystals formed after the glass transition. It is also important to note here that there exists some difference in the higher melting point of the initial film and the films crystallized from the melt. This is due to the solvent induced crystallization being operative when imidization is taking place. The enhanced mobility offered due to the solvent results in better packing and more perfect crystals. Secondly as the polymerization is not complete yet, the polyimide chains inherently possess a much greater degree of mobility thus enabling more perfect crystals (with respect to lesser defects inside the crystal lattice and a smoother surface-resulting in lower surface energies and higher melting points).

While this melting response is obtained after quenching from the melt, it is also important to understand the effect of varying cooling rates on subsequent melting behavior. Studying the effect of cooling rate also yields information on the crystallization kinetics of the polyimide. Figure 8.4 shows the heating scans after the polyimide was cooled from the melt at different rates. Decreasing cooling rates give the



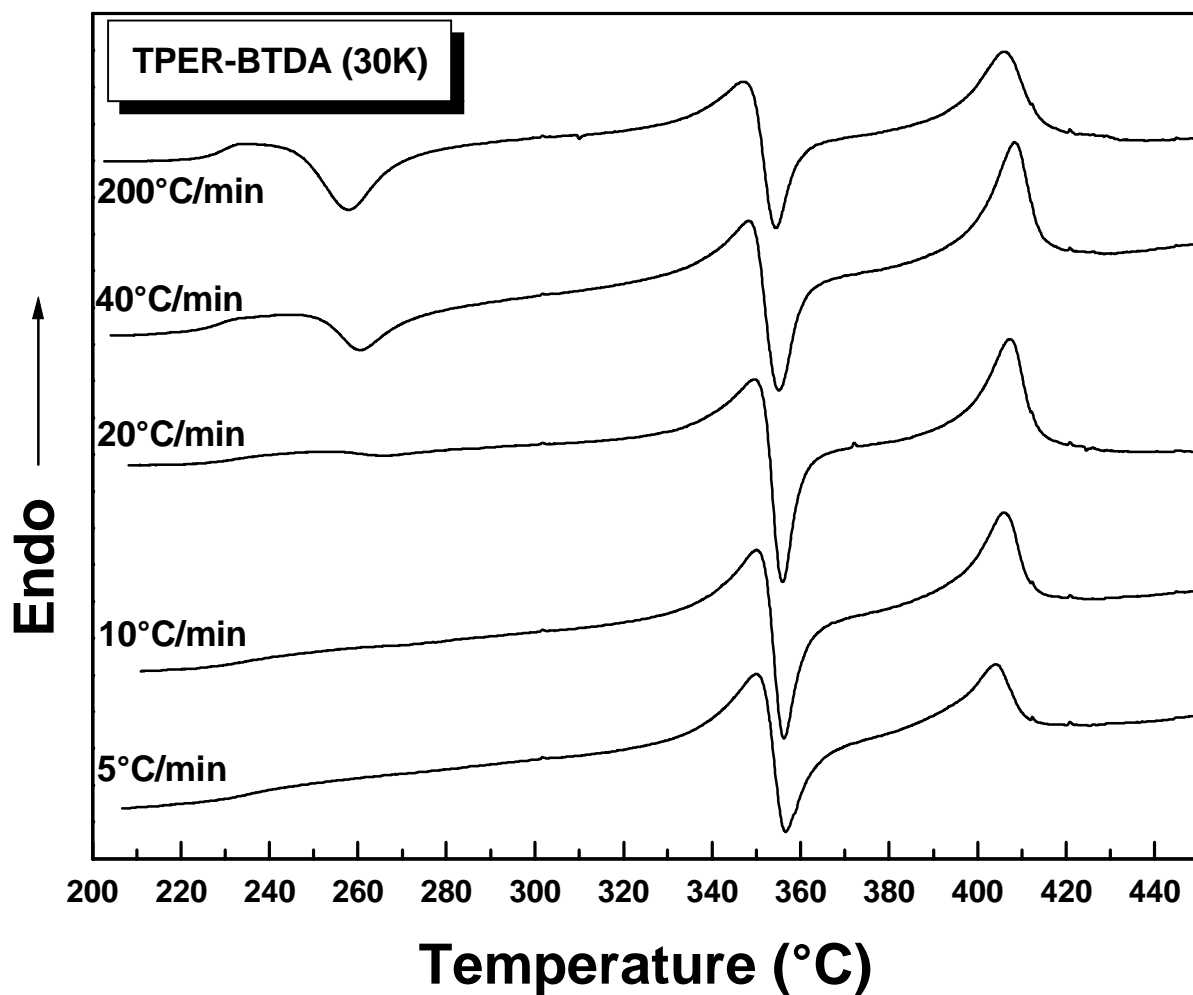


**Figure 8.4** Second heat DSC scans at 10°C/min after cooling from 450°C, 1 min at different cooling rates.

polyimide more time to crystallize during the cooling scan. This is clear from the glass transition behavior and the crystallization behavior after the  $T_g$ . The heat capacity jump at the  $T_g$  becomes relatively smaller and the magnitude of the crystallization exotherm after the  $T_g$  decreases tremendously as the cooling rate is decreased and the polyimide is given enough time to crystallize. Interestingly though, the nature of the lower melting endotherm does not appear to change much. It is also immediately succeeded by a sharp recrystallization exotherm that appears to broaden somewhat for slower cooling rates of  $5^\circ$  and  $10^\circ\text{C}/\text{min}$ . This is due to the extended time that the polyimide experiences at high temperatures for these slower cooling rates, and the corresponding increased crosslinking/chain-branching that may ensue in such a case. A corresponding decrease in the magnitude of the higher melting endotherm, which results from this recrystallization process, is also observed. *However, it is interesting to observe that the higher melting crystals always form during the prominent recrystallization process during the heating process and not during the cooling process (even when the cooling rate is slow).* The adjacency of the intermediate crystallization exotherm with the lower melting endotherm also suggests that the crystallization is distinctly associated with melting of the previous crystals. One of the reasons for this could be that the fast recrystallization occurs at sites of just melted crystals. This proposal is further discussed in subsequent sections.

Several reasons to elucidate the overall melting behavior can be offered, of which the three important ones are: (a) a *continuous melting-recrystallization model* to explain the lower melting endotherm and the higher melting endotherm (b) a *morphological model* with the two endotherms representing melting of lamellae with different thickness', the thicker lamellae being formed due to the recrystallization at the higher crystallization temperature (c) different crystal unit cell structures being responsible for the two melting endotherms with the crystal transformation taking place during the recrystallization step. Subsequent discussion in this chapter will consider the applicability of these various reasons in addressing the melting behavior in light of the available experimental evidence. However, before such an exercise is undertaken it is first important to recognize the effect of various isothermal crystallization temperatures on how they may influence the melting behavior.

Figure 8.5 (a) and (b) show the heating scans after the polyimide was melt crystallized at temperatures ranging from 270°C to 380°C after quenching from the melt at 450°C for 1 minute. This range of crystallization temperatures covers the temperatures much below the position of the lower endotherm, at the position of lower endotherm and recrystallization exotherm and also temperatures intermediate between the recrystallization exotherm and the higher melting endotherm. Figure 8.5(a) shows the scans from room temperature after crystallizing at temperatures ranging from 270-330°C, all of which are below the position of the lower melting endotherm. The characteristic melting behavior of this polyimide with two widely spaced melting endotherms and an intermediate recrystallization exotherm are clearly observed for all crystallization temperatures. However, a third melting shoulder appears ca. 15°C above the previous crystallization temperature. Such behavior has often been observed for a large variety of other semicrystalline polymers, though the magnitude of this shoulder in the present case is quite small. For other polymers exhibiting this behavior, the widely argued models again rest on either the ‘continuous melting and recrystallization’ or the ‘difference in morphology’ being responsible for lower melting shoulder and subsequent main melting endotherm. According to the melting-recrystallization model then, the lower melting shoulder would be due to the onset of the melting of the crystals formed at the crystallization temperature, after which a continuous melting and recrystallization process ensues. The lower melting endotherm at ca. 350°C then appears when the rate of melting exceeds the rate of recrystallization. The ‘morphological model’ ascribes the lower melting shoulder to the melting of thinner lamellae formed during the secondary crystallization while the main primary lamellae lead to the primary endotherm (in this case the lower melting primary endotherm at ca. 350°C). *This author believes that the ‘morphological model’ and not the ‘melting recrystallization model’ is more appropriate in describing the lower melting endotherm.* It is useful to notice here that the position of the lower melting peak shifts to slightly higher temperatures as the crystallization temperature is raised. Such a behavior is inexplicable on the basis of a continuous melting-recrystallization approach, which if true would have resulted in the melting temperature being the same. For example, if the continuous

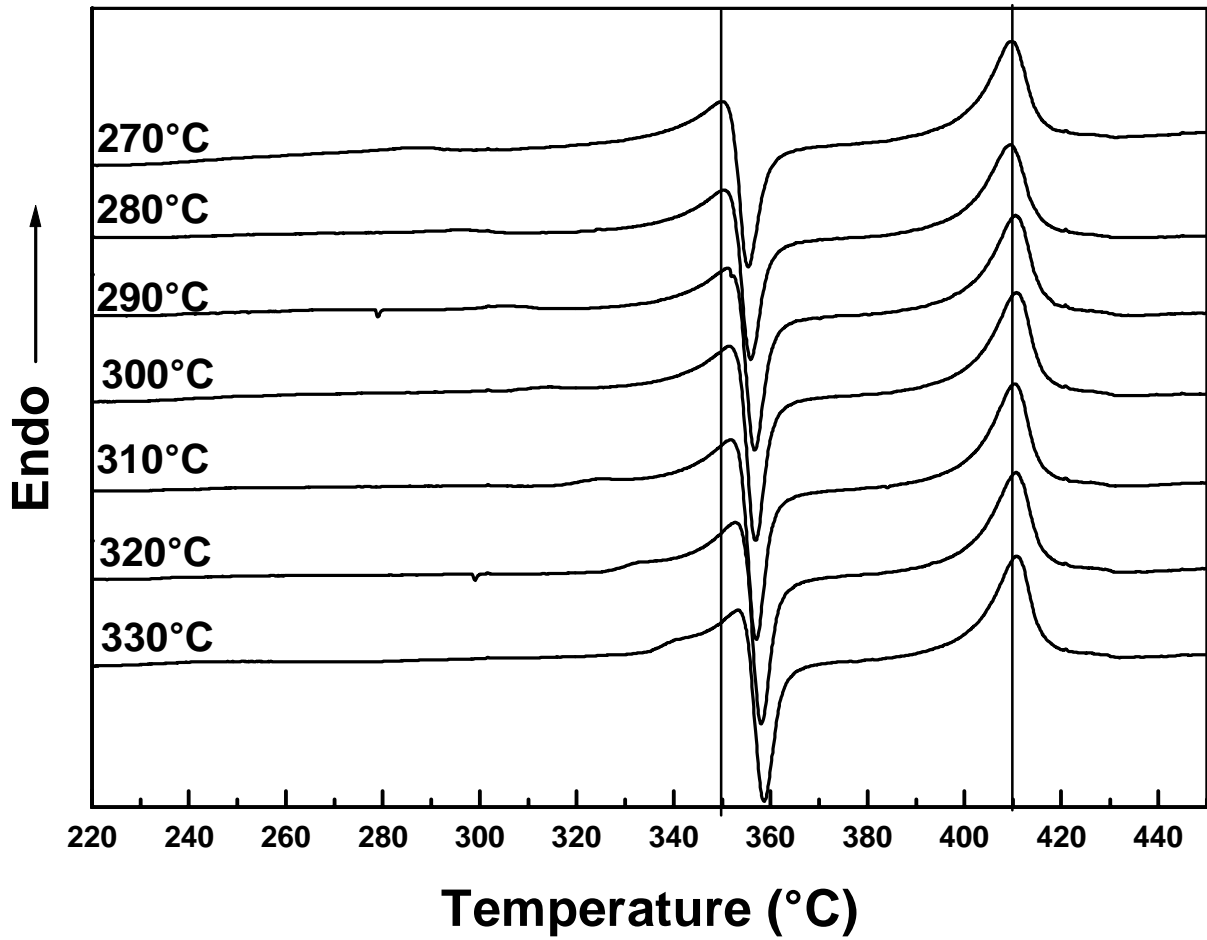


**Figure 8.5(a)** Scans from room temperature at 10°C/min after crystallizing at different temperatures from the melt at 450°C, 1min. Samples crystallized for 60 min.

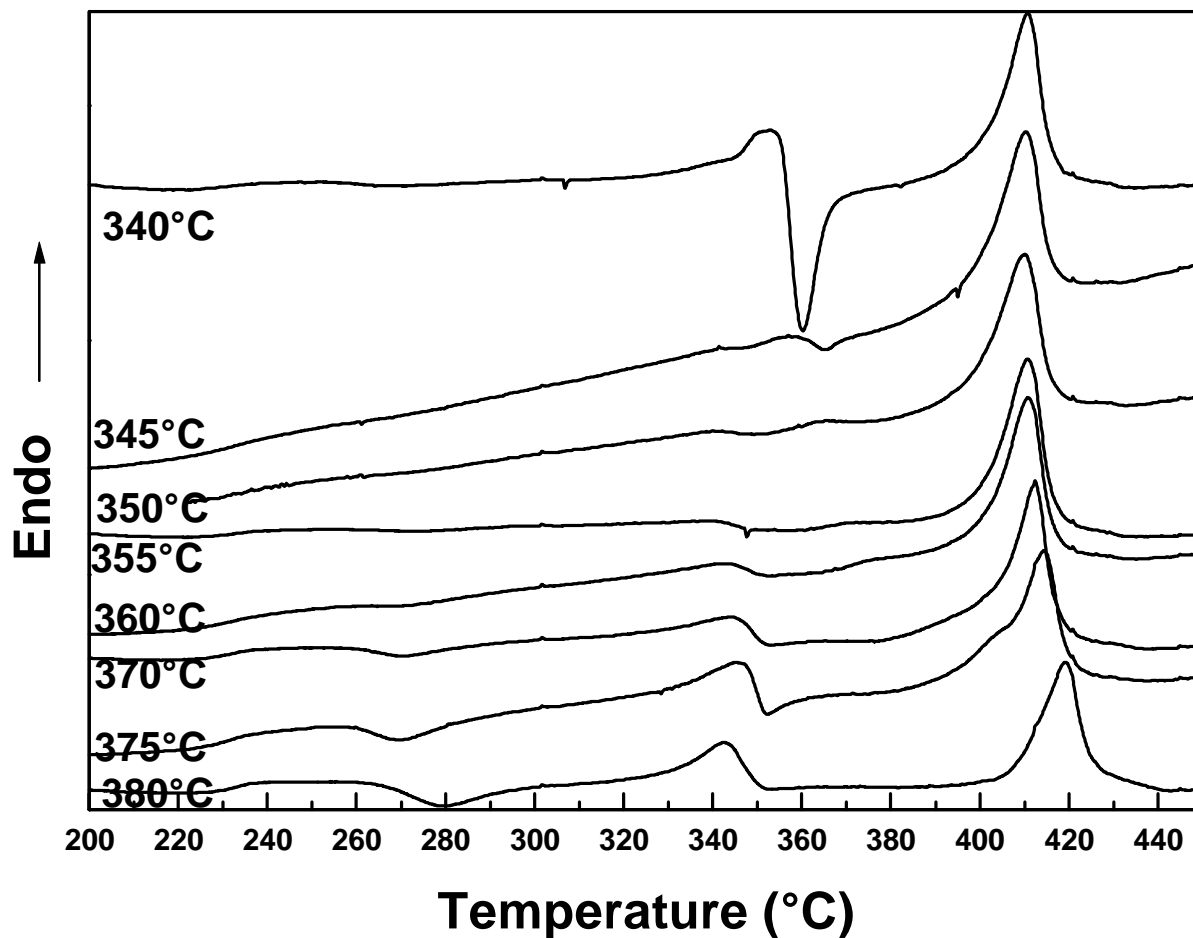


**Figure 8.5(b)** Scans from room temperature at 10°C/min after samples were melt crystallized at different temperatures and quenched to room temperature. The melt conditions utilized were 450°C for 1min. Samples for 340°C-360°C crystallized for 60 min. Samples for 370°C-380°C crystallized for 3 hours.

melting-recrystallization process was operative than the crystals formed at 270°C will start reorganizing at temperatures above 270°C. At a higher temperature then, say 330°C, these crystals should not be much different than crystals formed at 290°C (which start reorganizing above 290°C). The final melting temperature of the crystals then should have remained unchanged if such a phenomenon was taking place. These preceding arguments, however, rest on the assumption that kinetics of melting-recrystallization are faster compared to the heating rate utilized. This assumption usually holds good for the heating rate of 10°C/min utilized above. Other evidence supporting this conclusion (also from the DSC experiments) will be presented in the later sections.

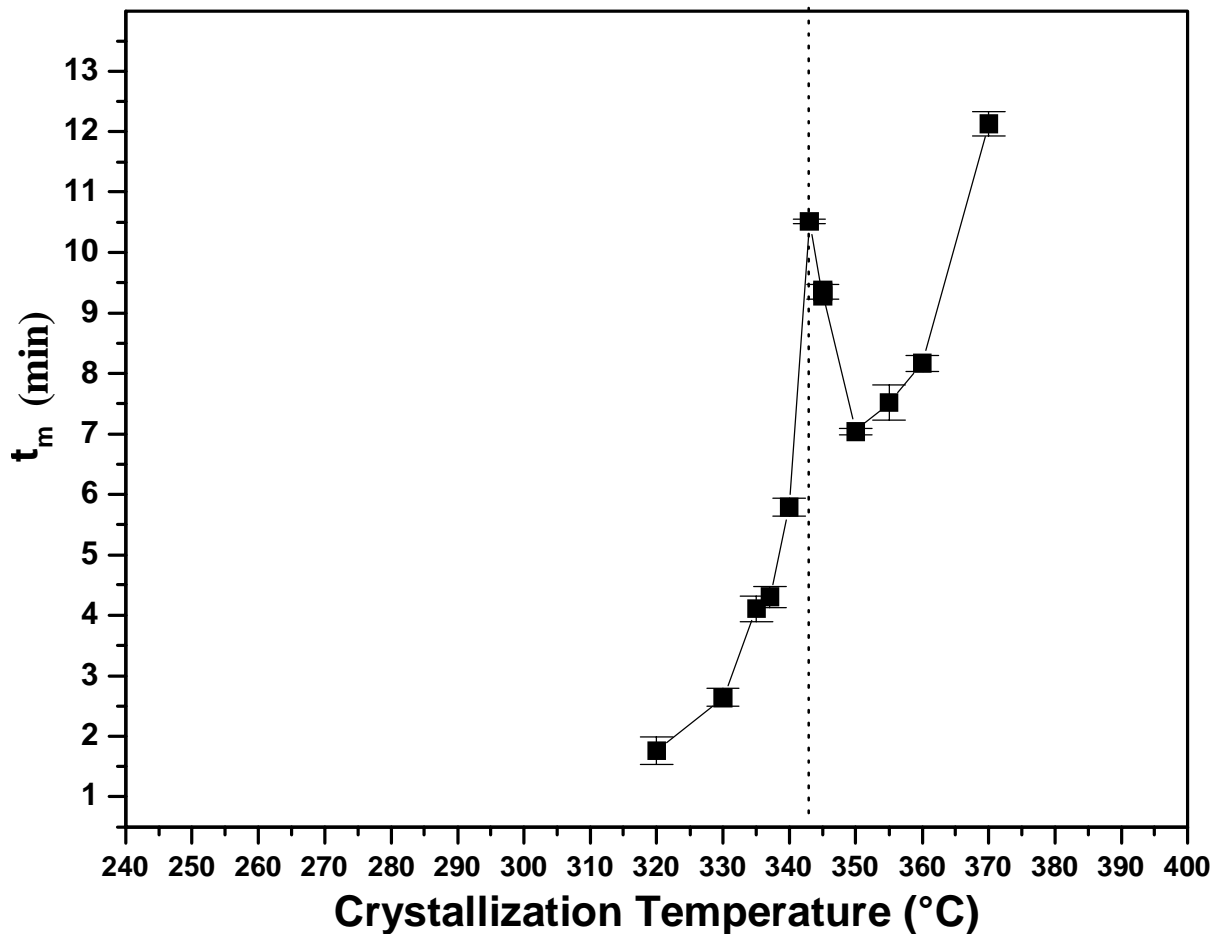
It also needs to be recognized that the position of the observed peak temperature for the lower melting endotherm may depend upon the subsequent recrystallization exotherm to some extent. This may occur due to the possibility of the recrystallization starting with the onset of the melting process. The DSC signal obtained in such a case then results from these two simultaneous processes. The shape of the overall melting and recrystallization behavior observed during the DSC scan thus depends upon the relative position of these two processes. In this regard, the recrystallization exotherm, which depends upon the melting of the crystals at ca. 350°C, also shifts to higher temperatures. The final melting endotherm at ca. 410°C is independent of the previous crystallization temperature for this range of  $T_c$ 's.

Figure 8.5(b) shows the heating scans after the samples are crystallized in the range 340°C-380°C. The lower melting shoulder that appears at ca. 15°C above the previous crystallization temperature occurs very close to the main lower melting endotherm for  $T_c=340^\circ\text{C}$ , while the melting behavior changes drastically as the crystallization temperature is raised just 5°C to 345°C. It is noticed that for a sample crystallized at  $T_c=345^\circ\text{C}$ , only a small endotherm at ca. 350°C is produced followed by immediate recrystallization and a final larger melting endotherm at ca. 410°C. This indicates that at  $T_c=345^\circ\text{C}$ , most of the crystals that form are those that melt at higher temperatures. The small population of lower melting crystals that result in the small endotherm at 350°C may form during the fast cooling to room temperature or during the heating scan from the room temperature. Similar behavior is obtained for  $T_c$ 's greater

than 350°C. In fact, for  $T_c$  greater than 360°C, a crystallization exotherm begins to appear during the heating scan resulting in formation of lower melting crystals. Also, the peak position of the higher melting endotherm begins to shift to higher temperatures as the  $T_c$  is increased to 380°C. For the  $T_c$ 's above 350°C, the presence of any  $T_c+15^\circ\text{C}$  endotherm is difficult to detect. This issue is elaborated in greater detail in the forthcoming sections where the isothermal experiments at 360°C are described. These overall results clearly illustrate the significant effect that small changes in  $T_c$  can have on the overall melting behavior. The peculiar-melting behavior, with two prominent endotherms, changes dramatically as the  $T_c$  is raised above 340°C. Indeed this has important ramifications from an application standpoint, where the polyimide may be used for example in high temperature adhesive and composite applications. The modulus of the material is expected to show dramatic changes at ca. 350°C for the samples which are crystallized below 345°C, while the modulus is expected to hold till much higher temperatures for samples crystallized above 340°C.

Another issue of significant importance is the crystallization kinetics at various isothermal temperatures. In this regard, the peak times for the isothermal crystallization exotherms are plotted in Figure 8.6 and give a good indication of the kinetics of crystallization at various temperatures. The data was obtained by utilizing a minimum of four experiments for each crystallization temperature and the average values of peak times as well as the error bars indicating the standard deviation are plotted. It is a well-established fact that when the crystallization takes place in the nucleation controlled region, the bulk crystallization rate increases as the degree of supercooling increases. In this regard, it is at first surprising to note the increase in peak crystallization times at intermediate crystallization temperatures. *This implies that the rate of crystallization starts to decrease with increasing supercooling in a narrow range of  $T_c$ 's close to 345°C!* These crystallization temperatures are close to the position of the lower melting endotherm. Also, as is previously discussed, melting behavior of the polyimide changes dramatically when crystallized at  $T_c$ 's above 340°C.

A likely reason for this peculiar behavior of crystallization half times is the presence of two crystal unit cell structures with different equilibrium melting points.



**Figure 8.6** Peak times for isothermal crystallization exotherms, after quenching from 450 $^{\circ}\text{C}$ , 1 min to different crystallization temperatures. The error bars indicate the standard deviation of at least four samples.



While the formation of lower melting crystals is favored at temperatures below 345°C, higher  $T_c$ 's promote the higher melting form. The rise in 'peak crystallization times' can then be explained due to a slower crystallization rate of lower melting crystals being formed at these temperatures. This slower rate is due to the lower 'effective supercooling' that is operative relative to the equilibrium melting point of these crystals. As the crystallization temperature is lowered further, the supercooling increases again and crystallization rate thus also increases. The peak crystallization times thus begin to decrease once more. During the heating scan the lower melting crystals, if present, completely melt at temperatures in the vicinity of 345°C-350°C and subsequently give rise to the higher melting form. In this case, the size of the recrystallization exotherm depends upon the size of the previous melting endotherm. This evidence and the immediacy of the recrystallization then suggest that the recrystallization process is closely associated with the previous melting of the lower melting form. It is possible to contemplate that only a small conformational rearrangement is needed of the chains constituting the lower melting crystals to give rise to higher melting crystals. Additionally, as there is relatively little melt disorder, the nucleation density 'in effect' is very high for the subsequent crystals to grow. This would then also explain the position and the fast rate of such a recrystallization process.

It is important to understand the morphological changes that may accompany this prominent bulk melting and recrystallization process. To this end, a hot stage polarized optical microscopy experiment was conducted where the polyimide was rapidly quenched from the melt to 340°C (where the low melting crystals form), crystallized at this temperature for 20 minutes and then *rapidly heated* to 370°C. A spherulitic morphology that appeared initially at 340°C, was then observed for any changes at 370°C. Also, a more severe melt condition of 460°C for 3 minutes was utilized to reduce the residual nuclei in the melt and thereby reduce the nucleation density at 340°C, thus facilitating easier observation. It was found that a very subtle and quick change occurred in the appearance of spherulites, when they were held at 370°C. This change is illustrated in Figure 8.7, where (a) illustrates the spherulitic morphology after 20 minutes at 340°C, and (b), (c) and (d) show the morphology at 370°C after 30s, 90s and 120s of holding

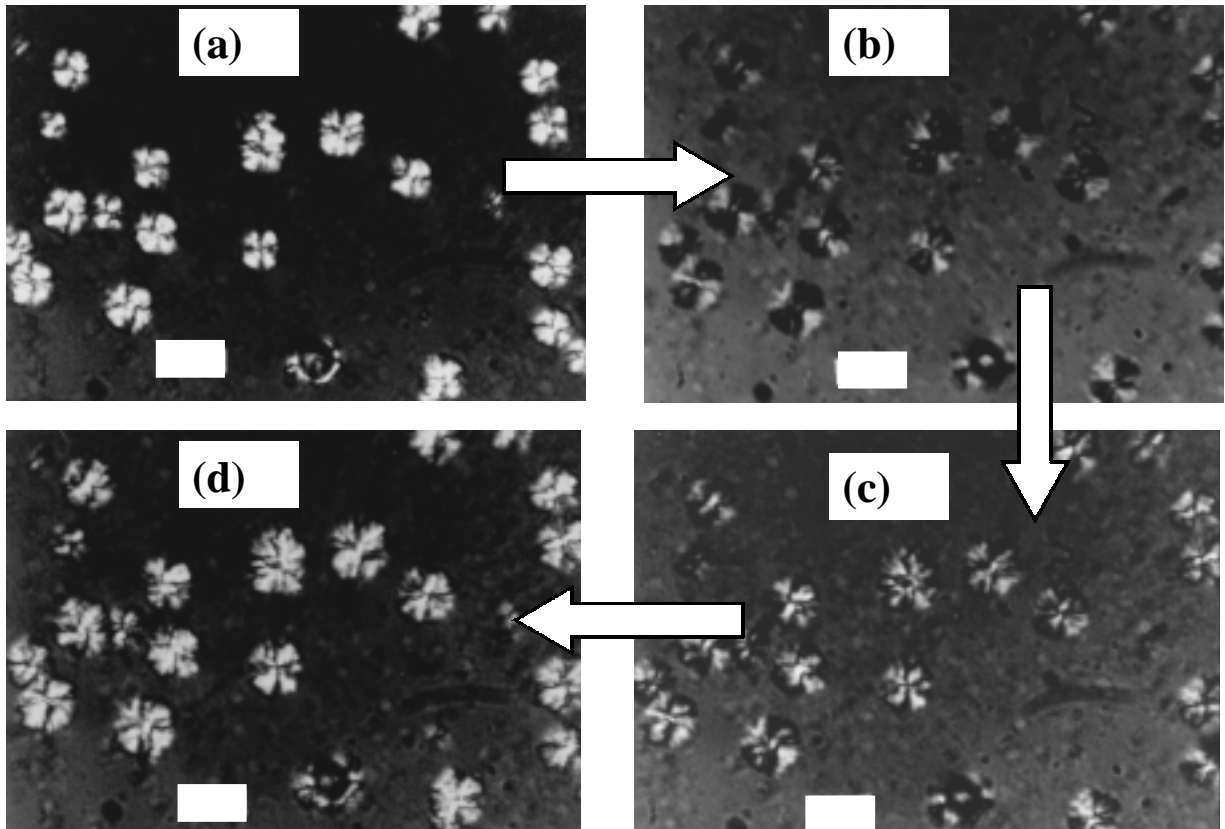


**Figure 8.7** Polarized optical micrographs of sample (a) crystallized at 340°C for 20 min and (b, c, d) held at 370°C for (a) 30s (b) 90s (c) 120s. The white scale bars indicate 25 microns.

time respectively. A coarse spherulitic morphology with only a weakly defined maltese cross is observed at 340°C. *However, when heated to 370°C, these spherulites consisting of low melting crystalline form, melt and give rise to new spherulites at exactly the same position.* The melting and recrystallization of the initial spherulites is illustrated in Figure 8.7 (b and c), where the birefringence first changes on melting (compare Figure 8.7(a) and Figure 8.7(b)). However, following melting, immediate recrystallization leads to the reemergence of spherulites that finally melt at ca. 410°C. If the temperature is held at 370°C, then the spherulites continue to grow at this temperature. In fact, from a polarized optical microscopy viewpoint, there is not much difference between the spherulites in Figure 8.7(a) and Figure 8.7(d), an observation also born out by independent experiments at these two temperatures. This evidence also explains to a large extent the reason for a sharp and adjacent recrystallization exotherm immediately after the lower melting endotherm. It also supports the earlier proposal of recrystallization occurring at or about the same sites with a possible conformational rearrangement of the chains to give rise to a different crystal unit cell structure.

Subsequently WAXD experiments were performed on samples crystallized above and below the temperature of lower endotherm to verify if any noticeable difference in the x-ray patterns was obtained. The WAXD scans in Figure 8.8 show the results obtained for the initial material, samples crystallized at 360°C and also for samples crystallized at 330°C. It is important to recall at this stage, that while the samples crystallized at 360°C and 330°C are expected to respectively contain only the higher and lower melting crystalline forms, the DSC results indicate that the as-received initial polyimide contains both the higher and lower melting form. However, for the samples crystallized at the three different temperatures, no significant differences are visible in terms of position of the peaks or presence of new ones. Thus this WAXD experiment is therefore not able to distinguish between the two different crystal unit cell structures, which may be due to the close similarity between them. Such similar WAXD scans have been reported for other materials that show two different crystal unit cell structures. It has been shown that although PET shows two different crystal unit cell structures (with different melting points), only very sharply resolved WAXD experiments (on isotropic

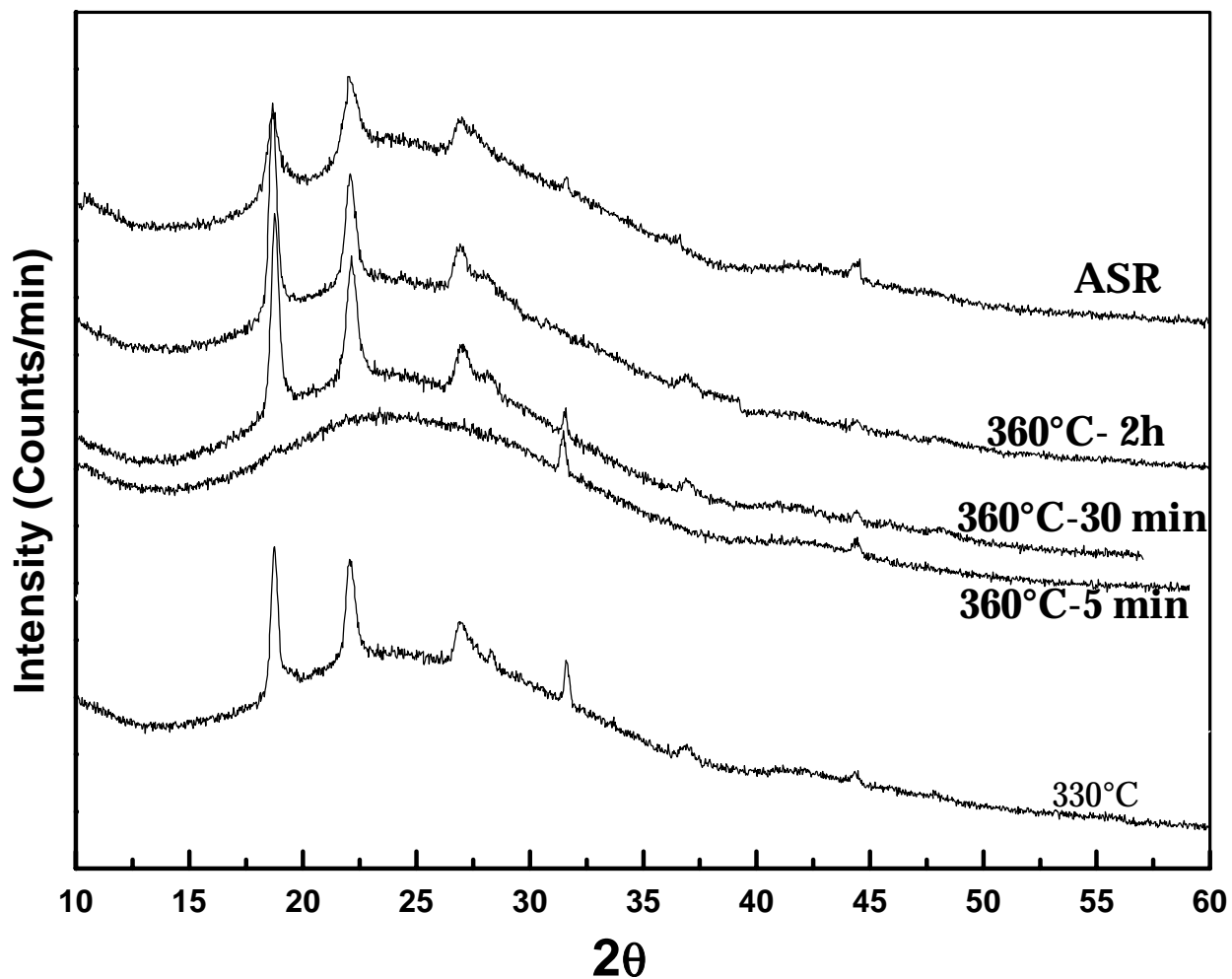


**Figure 8.8** WAXD patterns of TPER-BTDA-PA –initial film and melt crystallized at different temperatures. Samples were precisely prepared in the DSC.

samples) are able to resolve that difference. It is likely that the diffractometer utilized in this study did not resolve a small difference that might exist in the crystal unit cell structures of the present polyimide. A more detailed information regarding the crystalline reflections, possibly from a fiber pattern is required to resolve this difference. Thus in light of evidence demonstrated earlier, it is contended that the presence of two prominent and widely spaced endotherms is the result of difference in crystal unit cell structures, though it did not lead to different WAXD results for the isotropic films in the present study.

While two different crystal unit cell structures have been ascribed for the two prominent endotherms, it remains unresolved whether the crystals undergo a continuous melting and recrystallization process before the melting endotherms appear or the melting endotherms represent the melting of crystals formed at the previous crystallization temperature. Further experiments were hence conducted to resolve this issue and correctly surmise the cause of the two melting endotherms. In this regard two different types of experiments were conducted- one consisting of isothermal crystallization for varying times at the selected crystallization temperature and heating from that temperature, and the other consisting of scans of previously crystallized specimens at varying heating rates. Also, two crystallization temperatures, 320°C (below the lower melting endotherm), and 360°C (between the two endotherms) were selected for this purpose. The results from the isothermal experiments are discussed first to see if convincing evidence supporting either of the two models is obtained.

Figure 8.9(a) shows the direct heating scans from 320°C after the specimens were crystallized at that temperature for times indicated in the figure. A short residence time of only 1-minute at 320°C is unable to induce any crystallinity in the polyimide. Also, no additional crystallization occurs during the heating scan from that temperature though it takes 8 minutes (at 10°C/min) for the polyimide to reach the onset of the higher melting endotherm at 400°C. Possibly, any incipient nuclei, if formed, are destroyed as the temperature is continuously raised, thus precluding any significant crystallization (at this heating rate). Also, the progressive slowing down of crystallization kinetics with increasing temperature (see Figure 8.6) further lowers the possibility of any significant

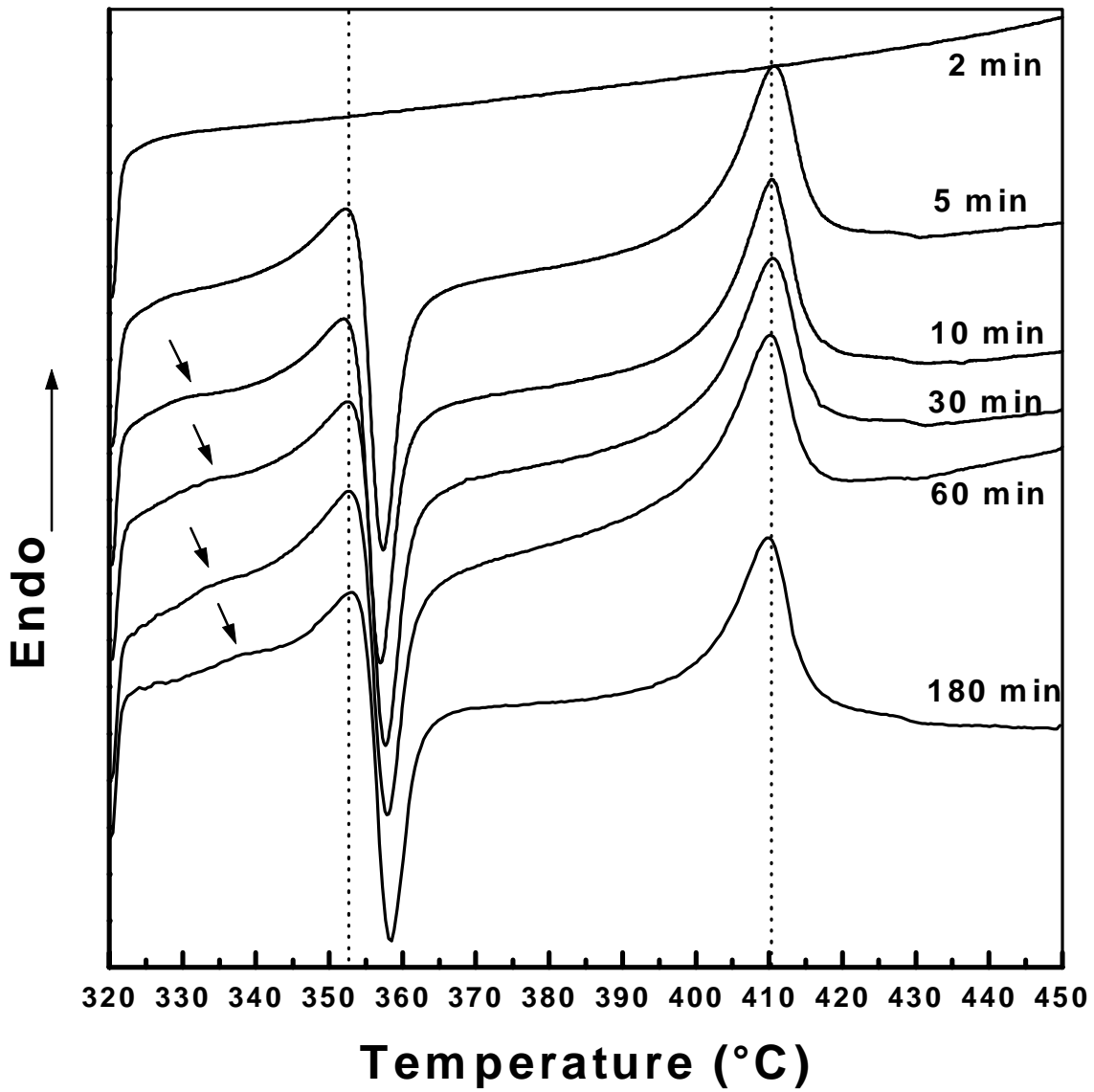


**Figure 8.9(a)** Direct DSC heating scans at 10°C/min after crystallizing for various times at 320°C.

crystallization occurring during the heating scan. However, crystallinity appears in the specimens for higher residence times of 5-180 minutes. No major changes, however, are observed between different specimens with respect to the position and size of the two prominent endotherms and the intermediate recrystallization exotherm. Additionally, a small but noticeable endotherm appears ca. 10-15°C above 320°C for times greater than 5 minutes, with its strength showing a small increase and its position slightly shifting to higher temperatures for increasing crystallization times. This is followed by the primary lower melting endotherm, whose peak position or size does not change with increasing time. There is a minor change in the position of the recrystallization exotherm that shifts to slightly higher temperatures. The higher melting endotherm, however, does not show any change in the peak melting point of 410°C.

The result that the main melting endotherm at ca. 353°C appears first and the much weaker melting shoulder at ca. 330°C later, suggests that the primary and first forming crystals at  $T_c=320^\circ\text{C}$  are responsible for the melting endotherm at ca. 353°C. The later forming thinner crystals due to secondary crystallization are then responsible for the weaker lower melting shoulder. The absence or relative weakness of the lower melting shoulder for shorter crystallization times is thus an argument in favor of the difference in morphology (with respect to the thickness of the crystals) being responsible for the lower melting shoulder and the melting endotherm at 353°C. If, however, the melting-recrystallization model is defended here, then a commonly utilized argument for explaining absence or weakness of the small melting shoulder is that at shorter crystallization times, the amount of crystallinity is low and hence the shoulder representing melting of such crystals is correspondingly weak/absent. This argument, however, does not hold here as the population of crystals melting at ca. 353°C is similar for all times (except 2 min) and thus the lower melting shoulder should also have been similar for all crystallization times. The higher melting endotherm at 410°C remains unaffected by the crystallization times at 320°C, as it only represents the melting of crystals formed during the recrystallization at 355-360°C.

The direct heating scans from 360°C, when the sample is crystallized for different times are also shown in Figure 8.9(b). In this case no additional lower melting shoulder

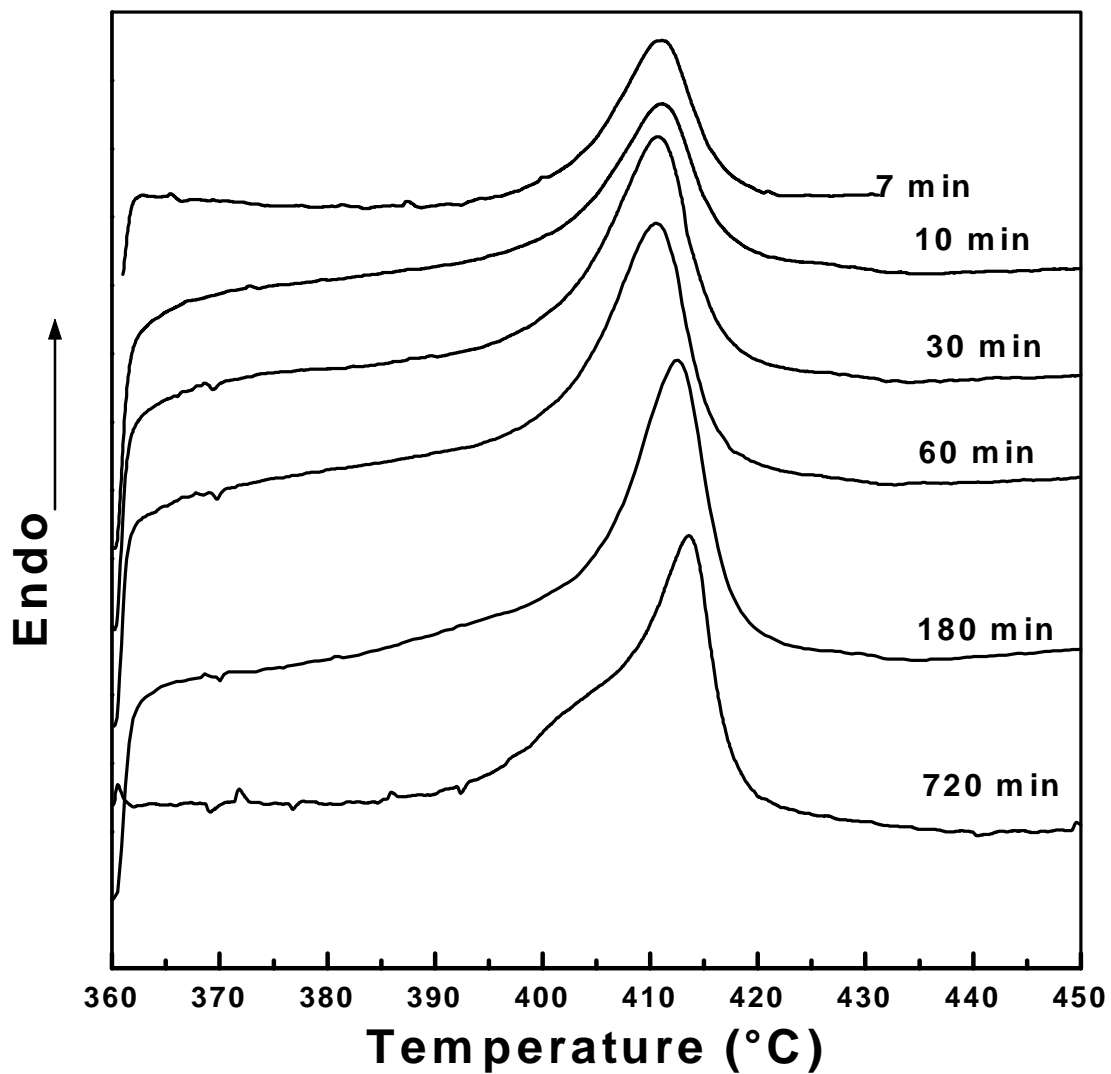


**Figure 8.9(b)** Direct DSC heating scans at 10°C/min after crystallizing for various times at 360°C.



is observed, but rather only a broad melting endotherm at ca. 410°C is obtained for all crystallization times. Also, for higher times of crystallization, the amount of crystallinity continues to increase (as indicated by the size of the endotherm) while a shift in the position of peak melting point is also observed. The absence of a well-defined smaller endotherm ca. 10-15°C above the crystallization temperature precludes assignment of the overall melting to either a 'continuous melting recrystallization process' or due to the 'melting of lamellae of two different thicknesses'. Rather it can only be said that a very broad melting population of crystals is obtained with the crystals starting to melt as the temperature is raised above 370°C.

To further substantiate the origin for the melting endotherms, experiments were conducted at varying heating rates for specimens originally crystallized at 320°C and 360°C respectively. Similar experiments were also conducted on the original as received polyimide film to detect any change in its melting behavior. Before conducting experiments at different heating rates, the DSC was carefully calibrated at each heating rate using zinc and tin standards. This minimizes any discrepancy in the DSC signal for varying heating rates although some error due to thermal lag effects may still result for faster heating rates. A lower weight of the samples was also used to minimize this error. Figure 8.10(a) shows the DSC scans for the initial film heated at rates ranging from 5-150°C. The overall shape of the DSC scan for the different rates does not change much and consists of the characteristic prominent dual endotherms and an intermediate recrystallization exotherm. It is important to note, however, that the position of the lower melting peak does not change with the heating rate. If this peak was the result of a continuous melting-recrystallization of previous crystals than the position of this peak is expected to shift to a lower temperature for faster heating rates, as lesser time is now available for the crystals to reorganize. Similar arguments can be extended for the behavior of the crystals associated with the higher melting peak, which also does not show much change in its position. Also, both the recrystallization exotherm and higher melting endotherm broaden somewhat as the heating rate is increased. It is, however, interesting to note that recrystallization process is not greatly reduced even for significantly faster heating rates of 80°C/min and 150°C/min, thereby indicating the

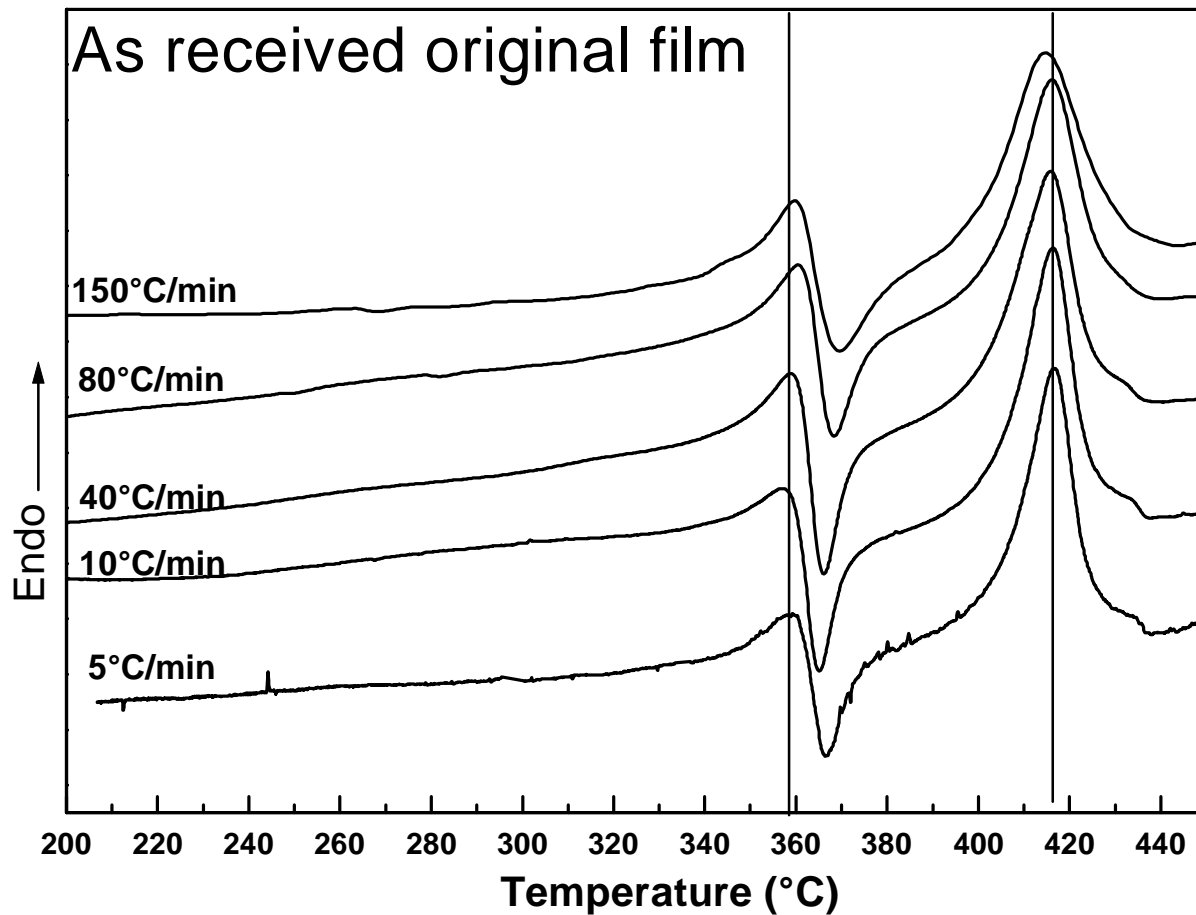


**Figure 8.10(a)** DSC heating scans at different heating rates for initial film after calibrating the DSC at different heating rates.

extremely fast kinetics associated with this process. It is also important to remember that the initial film undergoes a process of simultaneous polymerization and solvent aided crystallization during the synthesis process. The larger size of the higher peak clearly suggests that both higher and lower melting crystals form during the initial polymerization and simultaneous crystallization.

Figure 8.10(b) shows the DSC scans at different heating rates for films melt crystallized at 320°C for 1 hour-the crystallization temperature where only the lower melting form is expected to form. Expectedly the melting behavior is quite different from the initial film. Whereas the lower melting peak shows a slight shift to higher temperatures for faster heating rates, the size and position of the higher melting form depends significantly on the heating rate utilized. In fact, for the fastest heating rate of 150°C/min, the higher melting form is eliminated. This reduction in the higher melting form occurs concurrently with the reduction in the recrystallization process. It is interesting to note that although considerable broadening is visible for these two processes at faster heater rates, the peak position of the higher endotherm does not change much. This again contradicts the continuous melting-recrystallization being operative for the higher form, which if it had been true would have resulted in shifting of the higher melting peak to lower temperatures for faster heating rates. For the main lower melting peak at ca. 353°C, a lower melting shoulder discussed previously appears for the slower heating rates. If the lower melting shoulder represents the onset of the melting-recrystallization process, then it should gain strength (possibly even becoming a separate peak) and shift to higher temperatures for faster heating rates. Also, the main melting peak at ca. 353°C should shift to lower temperatures. None of these observations were made, thus indicating absence of a 'continuous' melting-recrystallization. The results can be readily explained on the basis of the 'morphological model'. The lower melting shoulder due to thinner crystals gets less defined due to the natural broadening of the melting for faster heating rates. The lower peak that represents the melting of primary crystals shows a slight shift to higher temperatures due to the delayed melting and small thermal lag. Hence, these results provide strong support for the difference in morphology being responsible for lower peak and a small shoulder associated with it.

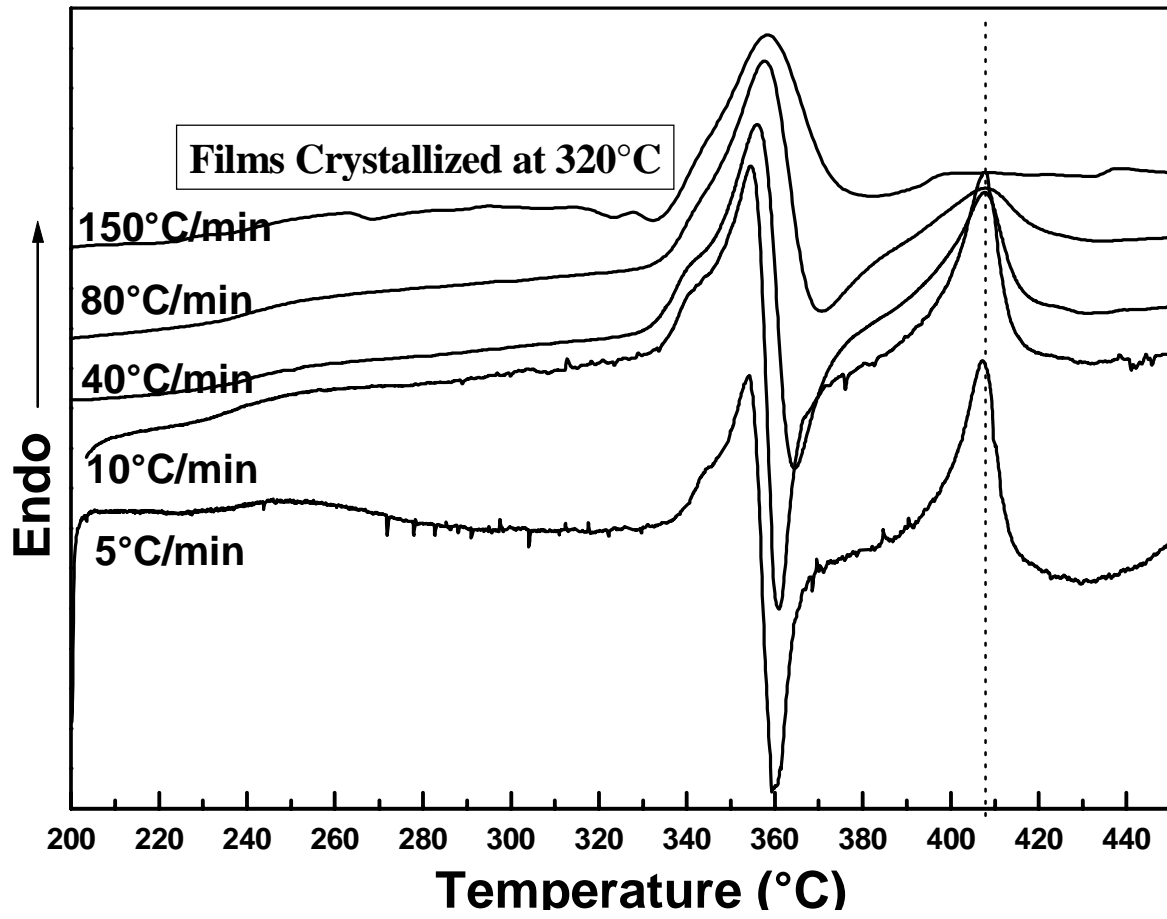


**Figure 8.10(b)** DSC heating scans at different heating rates for films crystallized at 320°C after calibrating the DSC at different heating rates.

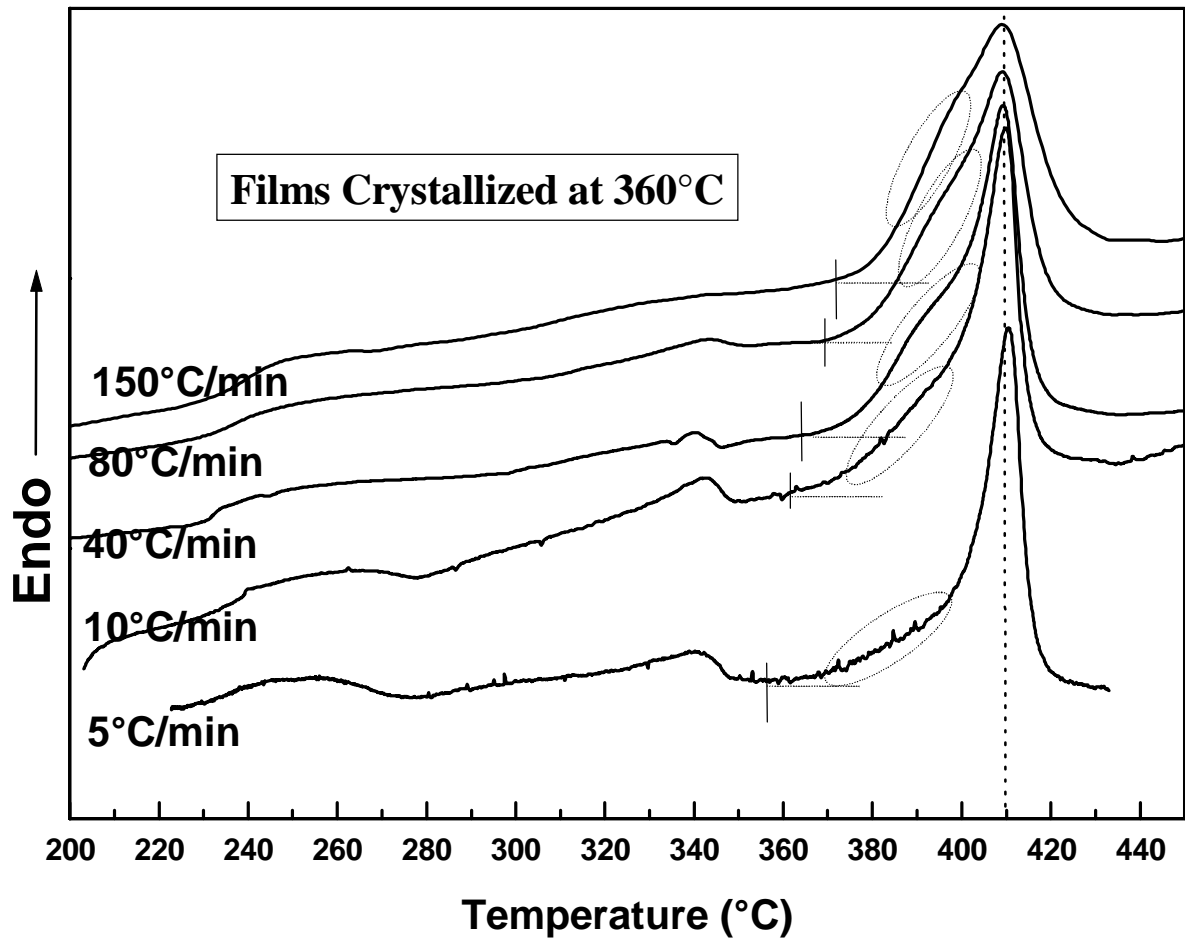


**Figure 8.10(c)** DSC heating scans at different heating rates for films crystallized at 360°C after calibrating the DSC at different heating rates. The encircled regions highlight the broad distribution of crystal thickness' which seems to broaden with increasing heating rate but does not become a separate peak in itself.

Figure 8.10(c) shows the DSC scans for polyimide crystallized at 360°C for 1 hr—a temperature where only the higher melting form is expected to form. The samples were quenched to room temperature before scanning at different rates. It is observed that while only one prominent endotherm at ca. 410°C is observed, a smaller endotherm at ca. 340°C appears for slower heating rates. The appearance of the lower endotherm is due to the crystallization that occurs above the glass transition temperature. Faster heating rates reduce this crystallization thereby resulting in a reduction of the melting endotherm at ca. 340°C. There is, however, no prominent recrystallization exotherm observed to give rise to higher melting crystals. It is useful to remember that this lower endotherm due to crystallization after  $T_g$  also occurred for  $T_c$ 's greater than 360°C. This suggests that there may be a population of chains that more easily crystallize into the lower melting form, but require much longer times to crystallize into the higher melting form when at crystallization temperatures that are greater than ca. 360°C. The higher melting endotherm broadens considerably as the heating rate is increased, although there is no effect on the peak position. It is also noted that there is a low temperature tail associated with the endotherms signifying the onset of melting of thinner crystals formed at 360°C. This melting starts after the temperature exceeds 360°C. The onset of melting seems to shift to slightly higher temperatures for faster heating rates due to delayed melting. The vertical bars drawn for various scans (Figure 8.10(c)) only roughly indicate the onset of this melting process rather than indicating its 'exact' position. For intermediate scanning rates, a shoulder appears on the low temperature side of the endotherm. However, this should not be identified as indicating the 'onset' for a continuous melting-recrystallization process (as has been done for other PEEK and other polymers by various workers). The author feels that this is a consequence of the natural broadening associated with faster heating rates. If a continuous melting-recrystallization process was occurring and the higher peak was a consequence of this process, than two events would have been taken place: (1) the lower melting shoulder would have tended to become a peak for faster rates (2) some shift to lower temperatures would have occurred for the higher peak. However, no such evidence supporting the continuous melting-recrystallization process is observed here. The effect of overall broadening of the various endotherms and

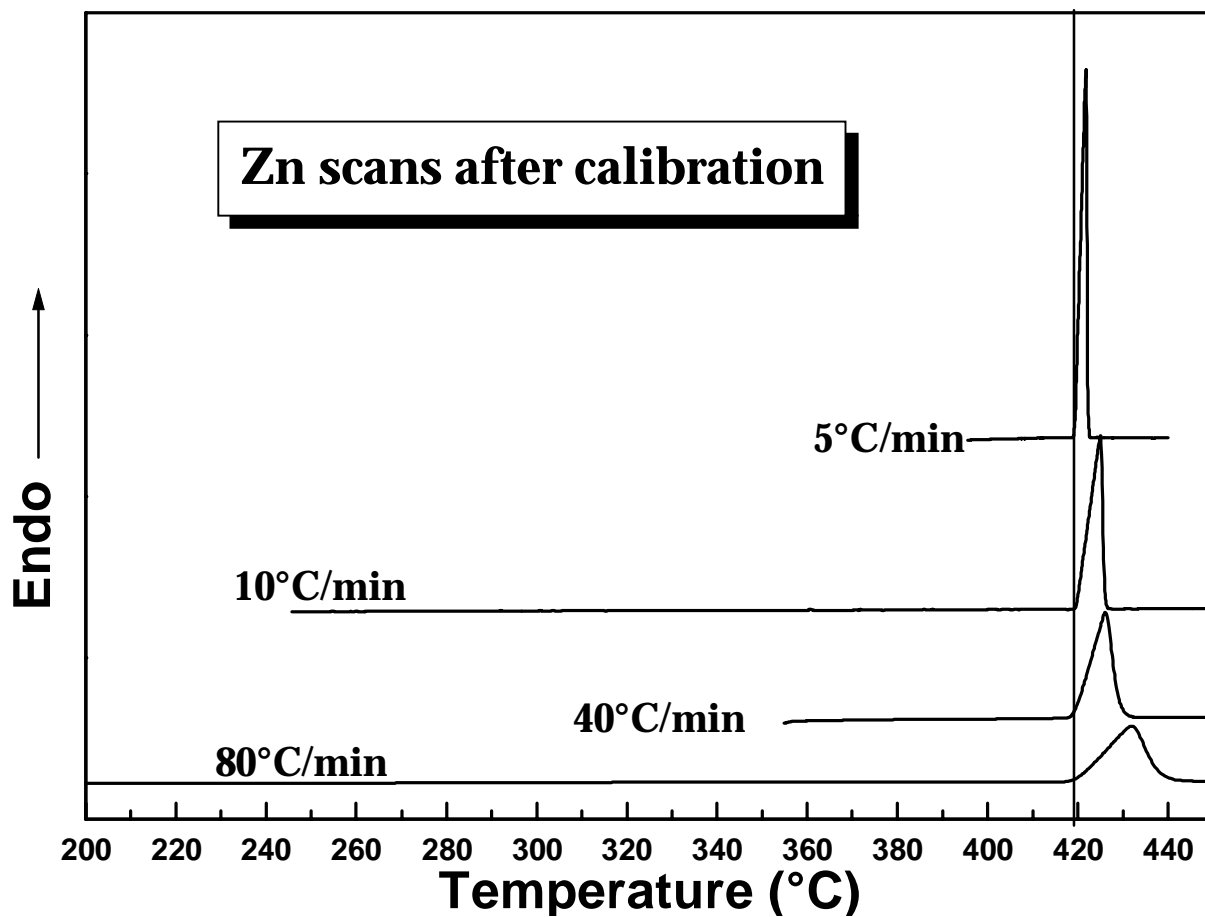


**Figure 8.10(d)** DSC heating scans at different heating rates for zinc after calibrating the DSC at different heating rates.

exotherms observed in Figure 8.10(a, b and c) is also shown for the zinc specimens in Figure 8.10(d) after calibrating at various heating rates. The onset of the melting point serves as a true measure of the calibration and is obtained to within 0.3°C for various heating rates. However, while a sharp peak is obtained for lower heating rates, the peak broadens for faster heating rates due to the thermal lag. Such an effect should be even more pronounced for the polymer samples and consequently a broadening is indeed observed in this case. However, it is surprising that the position of the various peaks do not show any major shift to higher temperatures for faster rates. This polyimide also demonstrates the commonly observed dependence of melting point on the previous crystallization temperature (see Figure 8.5(b)). For temperatures above 350°C, it is observed that higher  $T_c$ 's result in higher melting points.

It is earlier shown (Figure 8.9(b)) that there is some indication that the melting point of the polyimide crystallized at 360°C shifts to higher temperatures for longer times of crystallization. The increases in melting point can occur due to isothermal or non-isothermal thickening of the original crystals formed at 360°C. To further investigate this phenomenon, detailed experiments were conducted at 360°C and higher temperatures for longer crystallization times (Figure 8.11 and Figure 8.12). Also, the evolution of crystallinity was concurrently followed along with the variation in melting point as a function of time. Interestingly it was found that the melting point does not change much for residence times of ca. 100 minutes or less, while for longer crystallization times, a clear trend is observed in that the melting point increases as a logarithm of crystallization time. *In fact,, significant increases of 10-14°C in the melting point were observed for higher  $T_c$ 's and longer crystallization times.* It is also noted that these increases in melting point are not accompanied by any sharpening/narrowing of the endotherms and thus cannot be solely attributed to crystal perfection or narrowing of the crystal thickness distribution. Rather the endotherms at higher temperatures are broader indicating a wider distribution of crystal thickness with time. This phenomenon,, in the author's opinion, clearly reflects the 'crystal thickening' effects occurring at longer crystallization times in the polyimide. Also, there is an indication that the rate of thickening is faster for higher crystallization times, an observation commonly associated with such effects. However, it is peculiar to note that there seems to be an onset time associated with this crystal



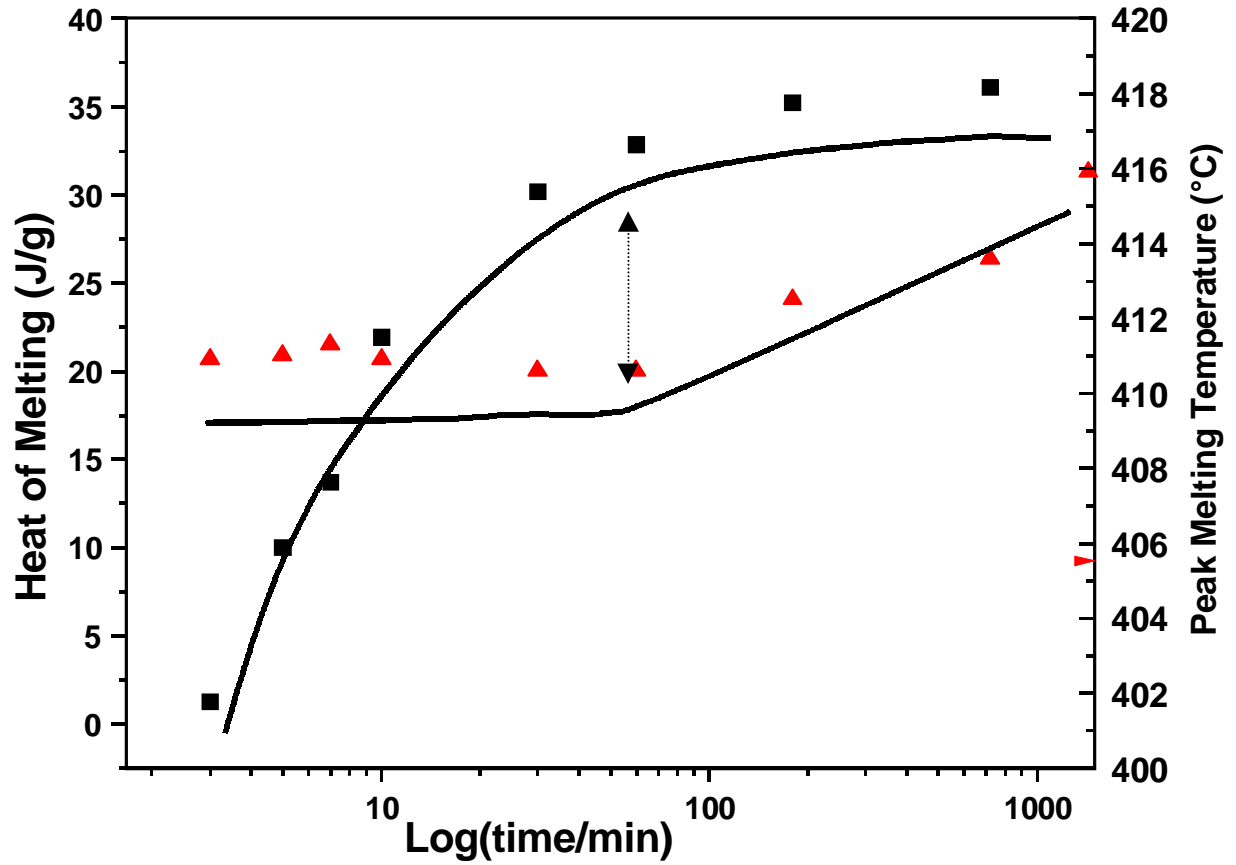


**Figure 8.11** Isothermal crystallization at 360°C with respect to logarithm of time (■) heat of melting obtained after heating to melt (▲) the corresponding peak melting points obtained.

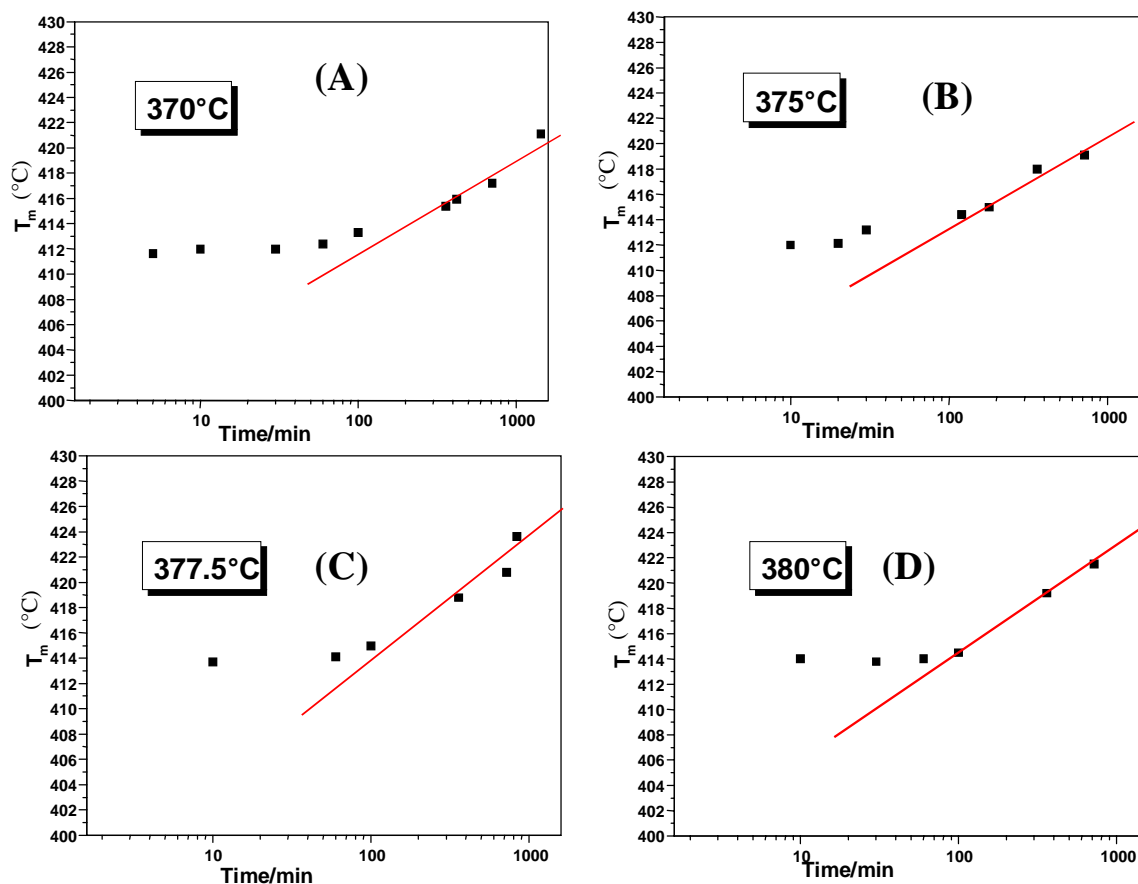


**Figure 8.12** Isothermal crystallization was carried out at various crystallization temperatures for varying amounts of time after quenching from the melt (450°C, 1min). The plots show the peak melting points obtained on heating with respect to the logarithm of the crystallization time. The crystallization temperatures for various plots are (a) 370°C, (b) 375.5°C, (c) 377.5°C and (d) 380°C.

thickening process. Figure 8.11 also shows the simultaneous evolution of crystallinity as indicated by heat of melting. For shorter times, the faster increase is associated with the primary crystallization process, while for longer times, the heat of melting begins to level off indicating the end of primary crystallization. It is important to note here that the onset of the thickening process is roughly associated with the ‘tapering off’ of the heat of melting curve. The results therefore suggest that the thickening phenomena depends somewhat on the end of the primary crystallization (see Figure 8.11). In this regard, it is relevant to first discuss the morphology of polyimide crystals. Other studies by this author using atomic force microscopy (AFM) and small angle x-ray scattering have indicated the presence of lamellar stacks within the material. However, the fold surfaces of these lamellae are not expected to be smooth. The long and semi-rigid nature of the chain will effectively block much adjacent or next neighbor reentry from taking place. It can therefore be conjectured that the nature of the fold surface is more akin to the switchboard model promulgated by Flory<sup>63</sup> and other workers<sup>64</sup>. While this model has remained controversial for polyolefins and other flexible polymers, it is more applicable for such rigid chain polymers as the one used in this study, which inherently cannot demonstrate a smooth and regularly folded surface due to their long repeat units and relatively more rigid chains. Thickening of the crystals then can take place by the incorporation of the segments adjoining the ones already crystallized. At times shorter than needed for the primary crystallization to be over, the amount of such thickening (which itself depends on primary crystals) is expected to be small. This can then explain the absence of any noticeable crystal thickening effect for shorter times.

Determination of the equilibrium melting point,  $T_m^\circ$ , is another aspect of fundamental importance in any crystallization study of a new polymer as it determines the undercooling dependence of the crystallization kinetics. This thermodynamic property determines the reference point for determining the driving force of crystallization and thus is also important when evaluating different crystallization theories, analyzing the spherulitic growth rates and nucleation density dependence. With respect to studying melt crystallization, it also determines the temperatures needed to erase the effect of previous thermal history and residual nuclei. In this regard, the

traditionally utilized method has been the Hoffman-Weeks analysis<sup>65</sup>, which results from the Gibbs-Thomson equation and an expression derived from Lauritzen-Hoffman theory<sup>65</sup>. However, this analysis, which was originally proposed for explaining the increases in melting points with crystallization temperature, is rigorously incorrect for predicting equilibrium melting points due to some fundamentally incorrect assumptions involved in its derivation<sup>67</sup>. Another popular method of determining the equilibrium melting point consists of fitting the spherulitic growth rate data at low undercoolings using the classical Lauritzen-Hoffman theory<sup>66</sup>. Also, Marand<sup>67,68</sup> et. al. have recently proposed a fundamentally more rigorous non-linear Hoffman-Weeks analysis for polyethylene and other flexible polymers which is better able to predict the equilibrium melting temperature. Most of these methods, however, depend directly or indirectly on the classical Lauritzen-Hoffman theory and its various modifications, which were initially derived for polyethylene and other flexible polymers. The successful application of the theory itself in modeling the crystallization of such rigid-chain and long repeat unit polymers is doubtful. This author's own application of Hoffman-Weeks analysis yields a very low equilibrium melting point of ca. 430°C for the present polyimide. This value is clearly erroneous as the end of the melting endotherm itself in many cases extends beyond this temperature. Also, the recently proposed non-linear method could not be successfully applied for this polyimide. The melting temperatures utilized for these analyses were based on the initial melting points where the absence of any significant thickening can be reasonably assumed. Others thermodynamic methods like the Gibbs-Thompson method and the Flory-Vrij method also cannot be easily utilized for determining the equilibrium melting point. The Gibbs-Thompson method<sup>65,69</sup> bases itself on presence of thin plate-like crystals where the lateral dimensions are significantly greater than the thickness of the crystals. This assumption is likely valid for the present polyimide (on the basis of independent AFM results). However, the lamellar thickness' at various  $T_c$ 's needs to be determined before such data, along with the melting data, is utilized to predict the equilibrium melting point using this analysis. Lastly, the Flory-Vrij method<sup>70</sup> requires preparation of a series of low molecular weight analogs. This demands synthesis and segregation of controlled molecular weight samples, an exercise not easy from a synthetic standpoint. Additionally, the molecular weight of the final polyimide is

difficult to determine (by conventional GPC analysis) due to insolubility of the final polyimide in common solvents.

#### **8.4 Conclusions**

This work introduces a new semicrystalline polyimide which is based on commercially available monomers. The polyimide displays high thermal stability both with regards to the TGA experiments and with respect to its ability to crystallize from the melt after repeated exposures to the high temperature of 450°C. A  $T_g$  of ca. 230°C, two distinct and widely spaced prominent melting endotherms at ca. 353°C and 416°C, and a prominent recrystallization process immediately proceeding the end of the lower melting crystals is evident. The two main crystallization endotherms are conjectured to be due to difference in crystal unit cell structures. The lower melting crystals form below ca. 350°C while the higher melting crystals form at higher temperatures. The abrupt increase in peak crystallization times (at ca. 340-345°C) is explained due to low supercooling experienced by the polymer at those temperatures with respect to the equilibrium melting point of the lower melting crystals. Hot stage polarized optical microscopy experiments reveal that the spherulites that develop at 340°C, melt and rapidly give rise to the higher melting spherulites at exactly the same site, when heated to 370°C. This also explains the occurrence of fast recrystallization exotherm immediately proceeding the lower melting endotherm. It is proposed that only a small conformational rearrangement is needed of the chains constituting the lower melting crystals (once heated above their melting point), to give rise to the higher melting crystalline form. The melting behavior depends significantly on the temperature of crystallization, with an additional low melting shoulder appearing 10-15°C above the crystallization temperature when crystallized at temperatures below the position of the lower melting endotherm. Only the higher melting crystals form at temperatures above 345°C leading to only one prominent melting endotherm at ca.410°C.

For specimens crystallized at 320°C, the primary lower melting endotherm appeared first and the lower melting shoulder developed only for later times. While the strength and the position of the primary lower endotherm does not change much, the shoulder shows a slight increase in strength and temperature of appearance. These results are concluded to support the 'morphological model' where the main lower melting endotherm is due to the melting of the first forming primary crystals and the weak lower melting shoulder is due to the secondary crystallization, which results in thinner crystals. Heating rate studies show that for specimens crystallized at 320°C, the lower melting shoulder becomes part of the primary lower melting peak with increasing heating rate. The main lower melting peak does not shift to lower temperatures with faster heating rates but rather shifts slightly to higher temperatures due to thermal lag. The recrystallization process after the lower melting shoulder that is responsible for the higher melting crystals weakens and finally disappears for faster heating rates. For specimens crystallized at 360°C, a broadening of the higher melting endotherm occurs. However, the peak temperature remains unaffected and does not move to lower temperatures for faster heating rates. It is thus concluded that for both kinds of specimens, the 'morphological model' is applicable. There does not seem to be any evidence which lends credence to a 'continuous melting and recrystallization' process being operative for this polymer. A similar conclusion is reached from the heating rate experiments on the initial film. An isothermal thickening phenomenon occurs at crystallization temperatures in excess of 350°C (giving rise to the higher melting crystals), as concluded from significant increases in melting points (10-14°C) for samples crystallized for longer times. There, however, is an induction time for start of this thickening phenomenon. This time corresponds roughly to the time needed for completion of the primary crystallization at different temperatures.

## Reference

---

<sup>1</sup> Hergenrother, P.M., Stenzenberger, H.D. and Wilson, D., *Polyimides*, Blackie & Sons Ltd., London, 1990.

- 
- <sup>2</sup> Mittal, K.L. and Ghosh, M.K., *Polyimides, Fundamentals and Applications*, Marcel Dekker Inc., 1996.
- <sup>3</sup> *Polyimides: Trends in Materials and Applications*, Ed. Feger, C., Khojasteh, M.M. and Molis, S.E., Proceedings of the Fifth International Conference on Polyimides, Ellenville, New York, Nov, 1994.
- <sup>4</sup> Ratta, V., Stancik, E.J., Ayambem, A., Parvattareddy, H., McGrath, J.E and Wilkes, G.L., *Polymer*, 1999, **40**, 1889.
- <sup>5</sup> Srinivas, S., Caputo, F.E., Graham, M., Gardner, S., Davis, R.M., McGrath, J.E. and Wilkes, G.L., *Macromolecules*, 1997, **30**, 1012.
- <sup>6</sup> Ratta, V., Ayambem, A., Young, R., McGrath, J.E. and Wilkes, G.L., *Polymer*, submitted for Publication, Nov, 1998.
- <sup>7</sup> Chang, A.C., Hou, T.H. and St. Clair, T.L. in *Polyimides: Trends in Materials and Applications*, Ed. Feger, C., Khojasteh, M.M. and Molis, S.E., Proceedings of the Fifth International Conference on Polyimides, Ellenville, New York, Nov, 1994, 3.
- <sup>8</sup> Sasuga, T., *Polymer*, 1991, **32**, 1012.
- <sup>9</sup> Tamai, S., Yamaguchi, A. and Ohta, M. *Polymer*, 1996, **37**, 3683.
- <sup>10</sup> Tamai, S., Oikawa, H., Ohta, M. and Yamaguchi, A. *Polymer*, 1998, **39**, 1945.
- <sup>11</sup> Graham, M.J., Srinivas, S., Ayambem, A., Ratta, V., Wilkes, G.L. and McGrath, J.E., *Polymer Preprints*, April, 1997, **38(1)**, 306.
- <sup>12</sup> Srinivas, S., Graham, M., Brink, M.H., Gardener, S., Davis, R.M., McGrath, J.E. and Wilkes, G.L., *Polym. Engg. Sci.*, 1996, **36**, 1928.
- <sup>13</sup> Mitoh, M. and Asao, K., *Polymeric Materials Encyclopedia*, **8**, 1996, 6220.
- <sup>14</sup> Holden, H.W., *J. Polymer Sci.* **6**, 1964, 53.
- <sup>15</sup> Mandelkern, L., Fatou, J.G., Denison, R. and Justin, J., *J. Polym. Sci. (B)* **3**, 1965, 803.
- <sup>16</sup> Bair, H.E., Salovey, R. and Huseby, T.W., *Polymer*, **8**, 1967, 9.
- <sup>17</sup> Harland, W.G., Khadr, M.M. and Peters, R.H. *Polymer*, **13**, 1972, 13.
- <sup>18</sup> Passingham, C., Hendra, P.J., Cudby, M.E.A, Zichy, Z. and Weller, M., *Eur. Polym. J.*, **26**, n6, 1990, 631.
- <sup>19</sup> Samuels, R.J. *J. Polym. Sci. (B)*, **13**, 1975, 1417.
- <sup>20</sup> Edwards, B.C., *J. Polym. Sci. (B)*, **13**, 1975, 1387.
- <sup>21</sup> Groeninckx, G. and Reynaers, H., *J. Polym. Sci. (B)*, **18**, 1980, 1325.

- 
- <sup>22</sup> Holdsworth, P.J. and Turner-Jones, A., *Polymer*, **12**, 1971, 195.
- <sup>23</sup> Qiu, G., Tang, Z., Huang, N. and Gerking, L. *J. Appl. Polym. Sci.*, **69**, 1998, 729.
- <sup>24</sup> Tan, S., Su, A., Li, W. and Zhou, E., *Macromol. Rapid Commun.* **19**, 1998, 11.
- <sup>25</sup> Woo, E.M. and Ko, T.Y., *Colloid Polym. Sci.*, **274**, 1996, 309.
- <sup>26</sup> Alfonso, G.C., Pedemonte, E. and Ponzetti, L., *Polymer*, **20**, 1979, 105.
- <sup>27</sup> Zhou, C. and Clough, S.B., *Polym. Eng. Sci.*, **28**, n2, 1988, 65.
- <sup>28</sup> Stein, R.S. and Misra, R.S., *J. Polym. Sci. (B)*, **18**, 1980, 327.
- <sup>29</sup> Nichols, M.E. and Robertson, R.E., *J. Polym. Sci. (B)*, **30**, 1992, 755.
- <sup>30</sup> Cheng, S.Z.D., Pan, R. and Wunderlich, B., *Makromol. Chem.*, **189**, 1988, 2443.
- <sup>31</sup> Yeh, J.T. and Runt, J., *J. Polym. Sci. (B)*, **27**, 1989, 1543.
- <sup>32</sup> Kim, H.G. and Robertson, R.E., *J. Polym. Sci. (B)*, **36**, 1998, 1417.
- <sup>33</sup> Qudah, A.M.A. and Raheil, A.A., *Polymer Int.*, **38**, n4, 1995, 375.
- <sup>34</sup> Chung, J.S. and Cebe, P., *Polymer*, **33**, n11, 1992, 2312.
- <sup>35</sup> Chung, J.S. and Cebe, P., *Polymer*, **33**, n11, 1992, 2325.
- <sup>36</sup> Lattimer, M.P., Hobbs, J.K., Hill, M.J. and Barham, P.J., *Polymer*, **33**, 1992, 3971.
- <sup>37</sup> Lee, Y., Porter, R.S. and Lin, J.S., *Macromolecules*, **22**, 1989, 1756.
- <sup>38</sup> Lee, Y. and Porter, R.S., *Macromolecules*, **20**, 1987, 1336.
- <sup>39</sup> Jonas, A.M., Russell, T.P. and Yoon, D.Y., *Macromolecules*, **28**, 1995, 8491.
- <sup>40</sup> Blundell, D.J., *Polymer*, **28**, 1987, 2248.
- <sup>41</sup> Blundell, D.J. and Osborn, B.N., *Polymer*, **24**, 1983, 953.
- <sup>42</sup> Cheng, S.Z.D., Cao, M.Y. and Wunderlich, B. *Macromolecules*, **19**, 1986, 1868.
- <sup>43</sup> Verma, R.K., Velikov, V., Kander, R.G. and Marand, H., *Polymer*, **37**, 1996, 5357.
- <sup>44</sup> Marand, H. and Prasad, A., *Macromolecules*, **25**, 1992, 1731.
- <sup>45</sup> Marand, H., Velikov, V. and Netopilik, M., *Polymer Preprints*, **34(2)**, 1993, 239.
- <sup>46</sup> Marand, H. and Velikov, V., *Polymer Preprints*, **34(2)**, 1993, 835.
- <sup>47</sup> Marand, H. and Velikov, V., *J. Therm. Anal.*, **49**, 1997, 375.
- <sup>48</sup> Verma, R., Marand, H. and Hsiao, B., *Macromolecules*, **29**, 1996, 7767.
- <sup>49</sup> Hsiao, B.S., Sauer, B.B., Verma, R., Zachmann, H.G., Seifert, S., Chu, B. and Harney, P., *Macromolecules*, **28**, 1995, 6931.
- <sup>50</sup> Hsiao, B.S., Gardner, K.H., Wu, D.Q. and Chu, B., *Polymer*, **34**, 1993, 3986.
- <sup>51</sup> Hsiao, B.S., Gardner, K.H., Wu, D.Q. and Chu, B., *Polymer*, **34**, 1993, 3996.



- 
- <sup>52</sup> Kumar, S., Anderson, D.P. and Adams, W.W., *Polymer*, **27**, 1986, 329.
- <sup>53</sup> Bassett, D.C., Olley, R.H. and Raheil, A.M.A., *Polymer*, **29**, 1988, 1745.
- <sup>54</sup> Kroger, K.N. and Zachmann, H.G., *Macromolecules*, **26**, 1993, 5202.
- <sup>55</sup> Deslandes, Y., Day, M., Sabir, N.F. and Suprunchuk, T., *Polym. Comp.*, **10**, 1989, 360.
- <sup>56</sup> Brandom, D.K. and Wilkes, G.L., *Polymer*, **36**, 1995, 4083.
- <sup>57</sup> Brandom, D.K. and Wilkes, G.L., *Polymer*, **35**, 1994, 5672.
- <sup>58</sup> Kreuz, J.A., Hsiao, B.S., Renner, C.A. and Goff, D.L., *Macromolecules*, **28**, 1995, 6926.
- <sup>59</sup> Hsiao, B.S., Kreuz, J.A. and Cheng, S.Z.D., *Macromolecules*, **29**, 1996, 135.
- <sup>60</sup> Sauer, B.B. and Hsiao, B.S., *Polymer*, **36**, 1995, 2553.
- <sup>61</sup> Hsiao, B.S., Sauer, B.B. and Biswas, A., *J. Polym. Phys.*, **32**, 1994, 737.
- <sup>62</sup> Harrison, I.R., *Polymer*, **26**, 1985, 3.
- <sup>63</sup> Yoon, D.Y. and Flory, P.J., *Faraday Discussions of the Chemical Society*, *n68, Organization of Macromolecules in the Condensed Phase*, 1979, 288.
- <sup>64</sup> Mandelkern, L., *Characterization of Materials in the Research: Ceramics and Polymers*, Syracuse University press, Syracuse, New York, 1975, 369.
- <sup>65</sup> Hoffman, J.D., Davis, G.T. and Lauritzen, J.I. *Treatise on Solid State Chemistry*, Ed Hannay, N.B., Plenum Press, New York, 1976, Vol. **3**, Chapter 7.
- <sup>66</sup> Hoffman, J.D., Frolen, L.J., Ross, G.S. and Lauritzen, J.I., Jr. *J. Research NBS Sect. A* 1975, **79**, 671.
- <sup>67</sup> Marand, H., Xu, J. and Srinivas, S., *Macromolecules*, **31**, 1998, 8219.
- <sup>68</sup> Marand, H., Xu, J., Agarwal, P. and Srinivas, S., *Macromolecules*, **31**, 1998, 8230.
- <sup>69</sup> Hoffman, J.D., *Polymer*, **32**, 1991, 2828.
- <sup>70</sup> Flory, P.J. and Vrij, A.J., *J. Am. Chem. Soc.*, **85**, 1963, 3548.